学位論文

The miR-199a/Brm/EGR1 axis is a determinant of anchorage-independent growth in epithelial tumor cell lines

（上皮がん由来の細胞株において、miR-199a/Brm/EGR1 axis は足場非依存性増殖に重要な役割を果たす）

平成 26 年 12 月博士（理学）申請

東京大学大学院理学系研究科

生物化学専攻

小林 和善

Abstract

In epithelial cells, miRNA-199a-5p/-3p and Brm, a catalytic subunit of the SWI/SNF complex, were previously shown to form a double-negative feedback loop through EGR1, by which human cancer cell lines tend to fall into either of the steady states, types 1 [miR-199a(-)/Brm(+)/EGR1(-)] and 2 [miR-199a(+)/Brm (-)/EGR1(+)]. I show here, that type 2 cells, unlike type 1, failed to form colonies in soft agar, and that CD44, MET, CAV1 and CAV2 (miR-199a targets), all of which function as plasma membrane sensors and can co-localize in caveolae, are expressed specifically in type 1 cells. Single knockdown of any of them suppressed anchorage-independent growth of type 1 cells, indicating that the miR-199a/Brm/EGR1 axis is a determinant of anchorage-independent growth. Importantly, two coherent feedforward loops are integrated into this axis, supporting the robustness of type 1-specific gene expression and exemplifying how the miRNA-target gene relationship can be stably sustained in a variety of epithelial tumors.

Table of Contents

Abbreviation List

BAF : BRG1-associated factor

BRG1 : Brahma-related gene 1

Brm : Brahma

CAV-1 : caveoline-1

CAV-2 : caveoline-2

ChIP : chromatin immunoprecipitation

Chr : chromosome

DMEM : Dulbecco's Modified Eagle's Medium

EGR1 : early growth response protein 1

EV : empty vector

FACS : fluorescence activated cell sorting

FCS : fetal calf serum

LNA : locked nucleic acid

miRNA : microRNA

NFκB : nuclear factor kappa B

NSCLC : non-small cell lung carcinoma

PBS : phosphate buffered saline

PCR : polymerase chain reaction

pre-miRNA : precursor miRNA

pri-miRNA : primary transcript of miRNA

RISC : RNA-induced silencing complex

RT-PCR : reverse transcription and polymerase chain reaction

SCC : squamous cell carcinoma

shRNA : short hairpin RNA

SWI/SNF : switch/sucrose-nonfermentable

TBS : tris buffered saline

TSS : transcription start site

UTR : untranslated region

VSV-G : vesicular stomatitis virus G protein

Introduction

Robust gene regulatory networks are required to maintain the identity of each cell types and several layers of regulatory molecular are involved in them. Among them, Chromatin remodeling factors play vital roles in epigenetical regulation via genome-wide gene transcription by modulating promoter activities[1]. On the other hand, microRNAs (miRNAs) are post-transcriptional regulatory molecules that suppress many target genes simultaneously to perform in diverse biological processes, including development, differentiation, and homeostasis[2]. Growing evidence indicates that the robustness of gene expression in specific cells is often supported by coordinated transcriptional and miRNA-mediated regulatory networks[3, 4]. In addition, improper use of these networks may lead to human diseases such as cancer. However, the interplay between chromatin remodeling factors and miRNA, as well as its biological outcome, is not fully understood in the context of gene regulatory networks common to a wide variety of cell lines.

I here concentrated on SWI/SNF complex, one of the major chromatin remodeling factor in human, and on miR-199a, which targets of Brm, a catalytic subunit of the complex, to elucidate gene regulatory networks formed in human cell lines originated from various epithelial tumors.

SWI/SNF complex

The human SWI/SNF-A complex (also known as the BAF complex), a member of a chromatin remodeling factor family composed of about 10 proteins[5] (Fig. 1), regulates gene transcription, either positively or negatively. Each SWI/SNF complex contains a single molecule of either Brm or BRG1 as ATP-dependent catalytic subunits, which have 75% amino acid identity[6], and regulates promoters of target genes. However, their target genes are not fully overlap and they show clear differences in their biological activities[7-10]. This complex cannot recognize specific DNA sequence, however, it is recruited to specific target promoters by interacting with various proteins, including transcriptional regulators, through many specific and varied associations with its several subunits or adaptor proteins[11]. For example, we have previously reported that the d4-family proteins DPF2 (REQ) and DPF3a/3b function as efficient adaptor proteins either for RELB/p52[12] and for RELA/p50[13] dimers to induce SWI/SNF-dependent NFκB target genes.

In terms of human cancers, SWI/SNF subunits functions have been reported to be often mutated in solid tumors suggesting that it can function as tumor suppressors[1, 11]. We and other groups have reported that Brm is frequently undetectable in various cancer cell lines[14], and in primary tumors of the lung[15], stomach[16], and prostate[17]. We

also found in nuclear run-on transcription assays that a functional *Brm* gene was present and actively transcribed in all of the Brm-deficient cancer cell lines tested[14, 18], indicating that Brm expression is largely suppressed by post-transcriptional gene silencing.

miRNA

miRNAs are short non-coding RNA of 20-25 nucleotide length and regulate gene expressions by posttranscriptional levels[19]. At present, more than 1800 miRNAs have been identified in the human genome (miRbase: http://www.mirbase.org/). The more than 30% genes encoding the protein are thought to be regulated by miRNA[20]. During miRNA biogenesis pathway[19, 21] (Fig. 2), a primary transcript of miRNA (pri-miRNA) is firstly transcribed by RNA polymerase Ⅱ in a similar way as mRNAs. The pri-miRNA is processed to precursor miRNA (pre-miRNA) by the RNase Ⅲ enzyme Drosha in cellular nuclei. Subsequently, the pre-miRNA is exported to the cytoplasm by Exportin5, and is processed by Dicer to produce the single stranded mature-miRNA. The mature miRNA is incorporated into RISC, and induce an inhibition of translation and/or degradation of the target mRNA following binding to 3' UTR of mRNA. Most miRNAs are evolutionarily conserved and play important roles various cellular processes[19]. Therefore, the dysregulation is involved with various diseases[22]. Especially, many

miRNAs are expected to be implicated in various cancer[23, 24]. Among these, miR-199a-5p and -3p have been extensively studied in many epithelial tumors. The precursor of miR-199a-5p and -3p are transcribed from two human genome loci; miR-199a-1 is present on chromosome (Chr) 19 and miR-199a-2 is present on Chr 1. The primary miR-199a-2 transcript includes miR-214 to form a miRNA cluster. Our previous study showed miR-199a-5p and -3p are mostly expressed from *miR-199a-2* genes at least in cell lines examined[25]. My preliminary data also show that pri-miR-199a-2 expression profile in the cell line panel tested in this study was very similar to those of mature-miR-199a-5p, -3p, and miR-214.

Brm/miR-199a/EGR1 axis

We previously found that both miR-199a-5p and -3p are directly involved in the post-transcriptional suppression of Brm. In addition, we reported that Brm negatively regulate transcription of *EGR1*. EGR1 in return, activates the transcription of *miR-199a (2)* gene locus. These findings suggest that, in the cell lines examined, Brm and miR-199a form a robust double-negative feedback loop that includes EGR1[25]. By examining a panel of human cell lines that were derived from a wide variety of cancer tissues, we previously found that they tend to fall into either of the steady states, miR-199(-)/Brm(+)/EGR1(-) cells and miR-199a(+)/Brm(-)/EGR1(+) cells[25], denoted

hereafter as type 1 and type 2, respectively.

The purpose of study

The early stage of our current study, we noticed clear differences in the biological properties between type 1 and type 2 cells: all of the type 1 cell lines tested (8 lines), but no type 2 cell lines (4 lines), have anchorage-independent growth activity. This activity has been well known to have good correlation to tumorigenicity *in vivo*[26]. Therefore, this result provides us with an unprecedented opportunity to unravel the robust regulatory networks involved in anchorage-independent growth common to these cancer cell lines. Of course, the gene expression patterns of each cancer cell line would be expected to be largely cell line-specific and dependent on a wide variety of factors, including the originating tissue type, mutated genes, and pathological properties, such as the tumor stage. However, I speculated that epithelial tumors would share regulatory networks that control their basic biological activities. In addition, I hypothesized that several genes would be specifically expressed in type 1 cancer cells, but not in type 2, and that they are regulated by Brm/miR-199a/EGR1 axis, and, further, that some of them would be crucial for their anchorage independency.

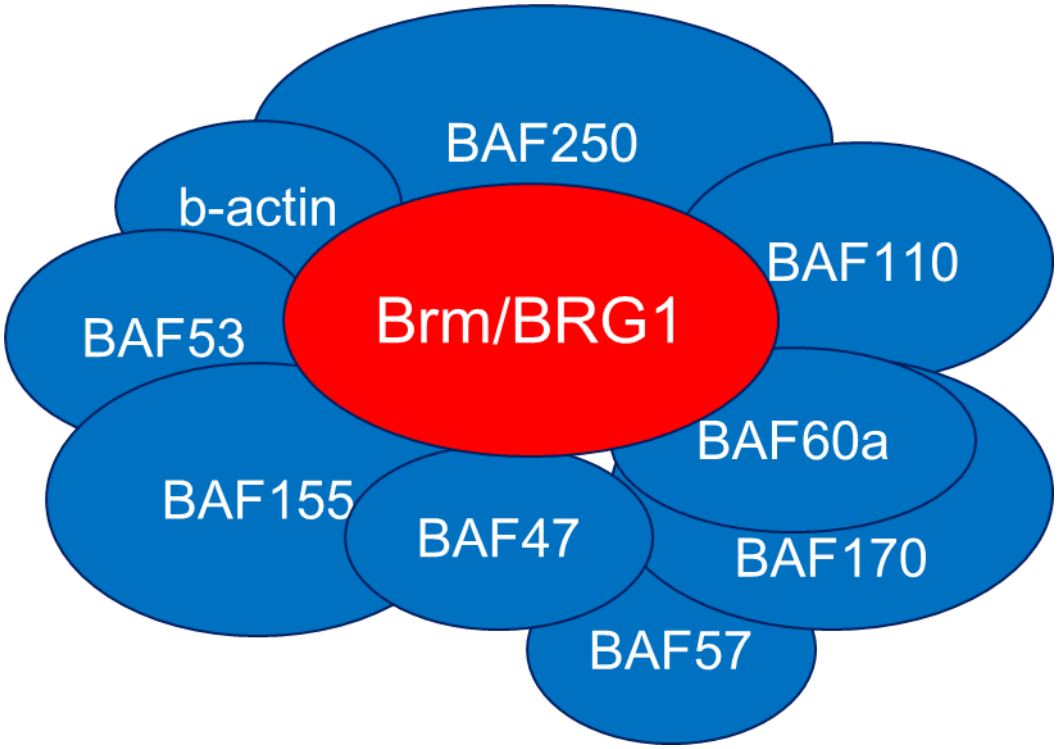

Figure 1. Schematic representation of the SWI/SNF complex. The SWI/SNF-A complex consist of about 10 proteins and remodels chromatin by using energy of ATPase. Each complex has either Brm or BRG1 as the catalytic subunit.

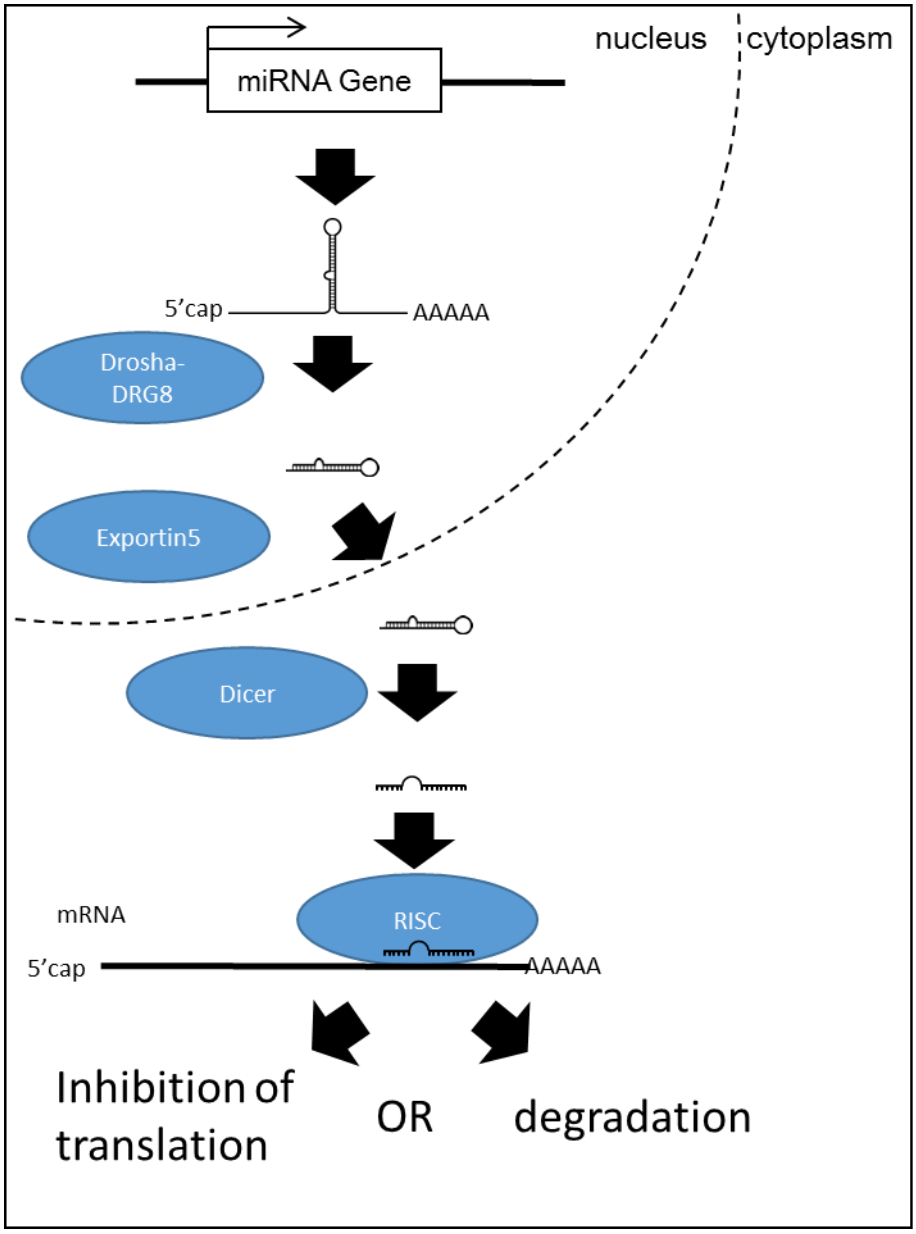

Figure 2. Biogenesis of the mature miRNA and its function

Results

Type 1, but not type 2, cells grow efficiently in soft agar

For type 1 and type 2 cells, I chose 12 cell lines (8 for type 1 and 4 for type 2) originating from various human epithelial tumors (Fig. 3). To ensure that I only examined cell lines originating from epithelial tumors, PA-1 (originating from tridermic teratocarcinoma), MDA-MB435 (recently discovered to originate from melanoma), and HEK-293FT (originating from human embryonic kidney) were removed from the panel of cancer cell lines previously used for categorization[25]. In addition, cell lines from one pancreatic (Panc-1) and three colon cancers (DLD-1, HT29, and HCT116) were added to the current analysis.

The results of a series of quantitative reverse transcription-polymerase chain reaction (RT-PCR) experiments (Fig. 3) confirmed our previous observations that epithelial tumor cell lines can be classified into two types according to the expression levels of Brm, EGR1, and miR-199a; type 1 cells specifically express *Brm* mRNA, whereas expressions of *EGR1* mRNA and miR-199a-5p and -3p, as well as miR-214, which is also generated from the *miR-199a (2)* gene locus, are restricted to type 2 cells. Notably, like *EGR1*, *EGR2*, *EGR3*, and *EGR4*, which are the other members of EGR family gene and which recognize the same DNA sequence[27], were shown to be type

2-specific (Fig. 3) by the parallel analysis. This might indicate EGR2, EGR3, and EGR4 are involved in the miR-199a/Brm axis in a similar manner to EGR1.

After several preliminary comparative analyses between type 1 and type 2 cells, I noticed clear differences in terms of anchorage-independent growth. Type 1 cells formed 25–300 colonies (more than 150 μm in diameter) in soft agar when 1,000 cells were seeded per 60 mm plate and kept for 21–28 days (Fig. 4). None of the four type 2 cells formed clear colonies in the same conditions. Notably, all of the type 2 cancer cell lines tested—SW13[28], HuTu80[29], H522[30] and C33A[31]—have shown clear tumor-forming activity in mouse xenograft models.

To test whether the anchorage-independent growth of type 1 cells requires Brm, I performed Brm knockdown experiments in several type 1 cells—A549, H1229, HeLaS3, and Panc-1—using a set of retroviral vectors containing shBrm (#4 and #5). I confirmed that all shBrm vectors significantly suppressed the levels of *Brm* mRNA and its product (see below) and that cells transduced with these vectors reduced colony-forming activity in soft agar when compared with that of negative control cells transduced with the shCre#4 vector (Fig. 5). These results reveal the pivotal role of Brm in anchorage-independent growth in type 1 cells. In several cases, strong suppression in colony formation in soft agar was observed by Brm knockdown, whereas the same

culture grow normally when kept in monolayer culture (A549 cells expressing shBrm#5 and HeLaS3 and Panc-1 cells expressing either shBrm#4 or #5, Fig. 6). In the case of H1299, however, I cannot exclude the possibility that reduction in the growth rate of monolayer culture partly contributed reduction in anchorage-independent growth. These findings provided us with an excellent opportunity to uncover the critical genes required for anchorage-independent growth of type 1 cells and suggested that these candidate genes would be expressed in a type 1-specific manner.

Several genes are preferentially expressed in type 1 cells

Whereas I know that suppression of the expression of a target protein by a certain miRNA is usually moderate and is not unconditionally retained in steady states, I selected the candidates of type 1-specific genes from various targets of miR-199a-5p (10 genes tested), miR-199a-3p (11 genes tested), and miR-214 (6 genes tested). These target genes were identified in previous reports or were predicted by target prediction algorithms as well as by our own analysis (Table 1). Of 32 candidate genes tested by quantitative RT-PCR (Fig. 7, 8, and 9), *CAV1*[32] and *KRT80* (both miR-199a-5p target genes) and *CD44*[33], *MET*[34], and *CAV2*[35] (all miR-199a-3p targets) were expressed in most of the type 1 cells but in none of the type 2 cells (Fig. 7). I also performed FACS

analysis for CD44 and MET using H1299 cells (type 1), and found that the entire population showed high levels of both CD44 and MET (data not shorn). I thus designated them as type 1-specific genes. Interestingly, two other epithelial-type keratin genes[36, 37], *KRT7*[38] (an miR-199a-3p target) and *KRT19* (an miR-199a-5p target), were not expressed in any of the type 2 cells but were expressed in some of the type 1 cells (Fig. 8 and 9).

The protein expression profiles of most of these type 1-specific genes, as well as four genes whose mRNA was expressed in both types, were examined by western blotting (Fig. 10) and relative amounts of each protein were quantified (Fig. 11). The protein expression profiles were generally very similar to those of the corresponding mRNA (Fig. 7). Mann-Whitney test further confirmed that these miR-199a target gene products (CD44, MET, CAV1 and CAV2) are specifically expressed in type 1 cells (Fig. 11). KRT80 protein was not analyzed because of the lack of a specific antibody. PTEN protein, a well-known miR-214 target, was clearly expressed in all of the cell lines except C33A cells, because C33A have homozygous nonsense mutation of this gene. It is noteworthy that among these type 1-specific proteins, CD44, MET, CAV1 and CAV2 function as plasma membrane sensors and signaling platforms and can be colocalized in caveolae in several physiological conditions[39].

A single knockdown of CD44, MET, CAV1, or CAV2 is sufficient to suppress anchorage-independent growth of type 1 cell lines

To evaluate whether the type 1-specific genes identified above contribute to the anchorage-independent growth of this cell type, I developed pairs of short hairpin RNA (shRNA) constructs for *CD44*, *MET*, *CAV1*, and *CAV2* capable of efficiently suppressing their target gene products (Fig. 12). Specific knockdown of KRT80 by shRNA was not possible because there are too many conserved regions among the large *keratin* gene family paralogues. After A549, H1299, HeLaS3, and Panc-1 cells were transduced with the shRNA-expressing retroviral vectors, their colony-forming activity in soft agar was evaluated (Fig.13). Single knockdown of *CD44*, *MET*, *CAV1*, or *CAV2* efficiently suppressed colony formation compared with negative control cells expressing shRNA for *Cre#4*. As an exception, the colony number of A549 cells expressing shCAV2#2 was slightly increased, probably due to off-target effects. Knockdown of *CD44*, *MET*, *CAV1*, and *CAV2* did not significantly affect cell growth. These results indicate that all of the four type 1-specific genes tested significantly contribute to the anchorage-independent growth of these type 1 cell lines.

All-or-none expression patterns of some type 1-specific genes in the cell line panel

are supported by two coherent feedforward loops that associate with the axis

Given that miRNA usually suppresses its target protein in a modest manner, it might be somewhat unexpected that some miR-199a targets were regulated in an all-or-none manner between type 1 and type 2 cells (Fig. 7 and 10). I speculated that this all-or-none phenomenon could be reflecting regulation by the molecular switch through miR-199a/Brm/EGR1 axis, where Brm and miR-199a expressions manifest a mutually exclusive pattern. Therefore, I first tested whether these type 1-specific genes, *CD44*, *MET*, *CAV1*, *CAV2*, and *KRT80* genes are under the positive control of the Brm-type SWI/SNF complex, for which type 1 cells are competent.

To test whether type 2 cells can induce type 1-specific genes when Brm is exogenously introduced, I transfected SW13 cells (type 2) with Brm expression plasmid or empty plasmid (EV1). In these experiments, some parallel cultures were cotransfected with the expression plasmids for representative NFκB dimers—RELA/p50 (canonical pathway) and RELB/p52 (noncanonical pathway)—or empty plasmid (EV2) to determine whether the activation is enhanced by NFκB dimers. As shown in Fig. 14, *CD44*, *MET*, *CAV1*, and *KRT80* mRNA were induced by Brm, as judged by quantitative RT-PCR, although the Brm induction effect varied among the genes. *CD44* and *CAV1* mRNA levels were increased by cotransfection with NFκB

dimers and Brm, whereas expression of *MET* gene was not NFκB dependent at all. *CD44* expression was more strongly dependent upon the noncanonical dimer RelB/p52 than RelA/p50, consistent with a recent report[40]. *CAV1* expression was further increased by cotransfection with RelA/p50 and Brm but was also significantly induced by RelA/p50 alone. Therefore, *CAV1* would only require Brm for its full expression. On the other hands, the expression levels of *GSK3β* and *Sirt1* (miR-199a-5p targets), and *PTEN* (a miR-214 target), which did not show type 1-specific expression patterns, were not affected by high levels of either Brm or NFκB in SW13 cells (Fig. 14). Next, A549, H1299, and HeLaS3 cells (type 1) were transduced with retroviral vector encoding Brm shRNA, and the steady-state expression of *CD44*, *MET*, *CAV1*, *CAV2*, and *KRT80* was evaluated by quantitative RT-PCR (Fig. 15a). The levels of *CD44*, *MET*, and *KRT80* mRNA were suppressed to various extents by Brm knockdown. Western blot analysis of parallel A549 cultures also indicated that *CD44* and *MET*, but not *CAV1* and *CAV2*, required Brm for expression (Fig. 15b)[8]. This strong Brm-dependency of CD44 expression is consistent with the previous report that assorted tissues from Brm null/BRG1-positive mice lack CD44 expression. Overall, these findings indicated that genes that are suppressed by miR-199a and simultaneously require the Brm-type SWI/SNF complex for efficient expression show distinct expression patterns:

expression in type 1 cells but no expression in type 2 cells. But *CAV1* and *CAV2* expression failed to show clear Brm dependency in A549 and H1299 cells.

I next tested whether type 1-specific genes are under the negative control of EGR1. When HeLaS3 and A549 cells were stably transduced with EGR1-expressing retrovirus, endogenous miR-199a-3p levels were elevated as expected from the axis (Fig. 16a). In HeLaS3, levels of *MET*, *CAV1* and *CAV2* mRNA (Fig. 16a) and their gene products (Fig. 16b and Table 2) were reduced by exogenous EGR1 expression. In the case of A549 cells, slight reduction of *CAV1* and *CAV2* mRNA and reduction of MET, CAV1 and CAV2 proteins were observed (Fig. 16a, b and Table 2). These results are consistent with previous reports indicating that *MET*[41] and *CAV1*[42] genes are negatively regulated by EGR1: the *MET* and *CAV1* promoters have one and three EGR/SP-1 binding sites, respectively. I also found EGR1 binding sites on the *CAV1*, *CAV2* and *MET* promoter regions (from -1600 to +500bp of TSS) by using ChIP-seq data obtained by ENCODE. These results suggest that *CAV1/2* and possibly *MET* are specifically expressed in type 1 cells by evading transcriptional suppression by EGR1 proteins and also post-transcriptional suppression by miR-199a-5p/3p.

Overall, these results suggest that there are at least two feedforward loops. One is composed of miR-199a-5p/3p, Brm and CD44, MET and KRT80 (Fig. 17a left) and

another is composed of EGR1, miR-199a-5p/-3p and CAV1, and CAV2 (and possibly MET) (Fig. 17a right). Type 1-specific genes would be regulated in an all-or-none manner by either of these two feedforward loops that associate with the robust miR-199a/Brm/EGR1 axis that dictates cancer cell lines to either of the steady states, [miR-199(-)/Brm(+)/EGR1(-)] and [miR-199a(+)/Brm(-)/EGR(+)] (Fig. 17b).

The miR-199a/Brm/EGR1 axis persists in an extended panel of cell lines originating from epithelial tumors

Because our panel of cancer cell lines used for the development of the cell line typing was limited to 14 cell lines, I intended to increase the number of cell lines by directly performing quantitative RT-PCR of *Brm* mRNA (using totally 4 PCR primer pairs), *EGR1* mRNA (using totally 4 PCR primer pairs) and miR-199a-3p by adding 12 new cell lines using the same experimental protocol as used for Fig. 3 (Fig. 18). The 4 independent PCR primer pairs for *Brm* or *EGR1* gave essentially the same expression profile, respectively (Fig. 18). Out of the total 26 cell lines, 23 could be categorized as either type 1 (17 lines) or type 2 (6 lines), according to the criteria shown in Table 3. The remaining 3 cell lines, which were originated from gastric carcinomas and mammary tumors, cannot be categorized into either type 1 or type 2 (designated type 3).

These results indicate that the miR-199a/Brm/EGR1 axis is largely retained in variety of epithelial tumor cell lines.

Since microarray data of *Brm* and *EGR1* mRNA for 17 among these cell lines categorized as type 1 and type 2 were available from Sanger database (Genomics of Drug Sensitivity in Cancer http://www.cancerrxgene.org), and their expression profiles obtained from the database was compared with those of the quantitative RT-PCR data shown in Fig. 19. I found that the expression profiles of *Brm* and *EGR1* are not correlates well between them. Since *Brm* mRNA levels of even Brm-deficient cell lines such as SW13, H522, C33A, A427, and H23—previously reported by our[7, 14] and other groups[8, 43] by RT-PCR or Northern blotting analysis—were significantly high according to Sanger database, there would be limitations in microarray data to estimate mRNA levels of such transcriptional regulatory genes as *Brm* and *EGR1* accurately.

Since we found expression profiles of *CD44*, *MET*, *CAV1* and *CAV2* mRNA by our quantitative RT-PCR and those obtained from Sanger Database are correlated well, I showed both of them in Fig. 20. The expression levels of *CD44* and *MET* were high in type 1 cell lines, whereas they were mostly undetectable in the type 2 cell lines even in these extended panels, and specific *CD44* and *MET* expression in type 1 cells were statistically supported in both data of quantitative RT-PCR and the Database. *CAV1* and

CAV2 expression was not detected in most type 2 cells with a clear exception of A427. Because of this, type 1 specific expression of *CAV1* and *CAV2* was not supported statistically. Relatively low *EGR1* expression in A427 among type1 cells (Fig. 18, Table 3) might partly explain this exception.

Expression patterns observed in type 1 or type 2 cell lines are recapitulated in some cancer lesions of NSCLCs

I finally examined whether the distinct expression patterns observed between the two cell types are reflected in human primary tumors. Since the cell lines originating from NSCLCs in the cell line panel used here can be categorized as both type 1 and type 2 (Table 3), I pathologically analyzed surgically resected, formalin-fixed, paraffin-embedded tissues from human cancer lesions of NSCLCs. Among NSCLCs, I especially focused upon squamous cell carcinoma (SCC), because in this type of cancer, we can easily understand activity of proliferation or the status/direction of differentiation two-dimensionally in the histological section. After preparing sequential thin sections of total 21 SCC cases, they were immunohistochemically stained with antibodies against Brm, CD44, MET, and CAV1 and also probed for miR-199a-5p by *in situ* hybridization and interrelationships among their expression patterns in the

coincident area of the each section were analyzed by comparing lower and higher differentiation status.

In the area of lower differentiation status where cancer cells are crowded by the active proliferation and have increased nuclear/cytoplasmic ratio without keratinization, I clearly observed a Brm^+, $CD44^+$, MET^+, and $CAV1^+$ phenotype in almost all cases. In some of these areas, expression of miR-199a was undetectable as shown in Fig. 21 (surrounded by solid line), which recapitulates the expression patterns of type 1 cells. However, in the other areas expressing these 4 proteins, I detected also miR-199a expression, indicating expression heterogeneity in cancer legions.

As for the areas of highly differentiation status, I observed them in many so-called cancer pearls in 4 cases of SCC, where cancer cells are sparse with large cytoplasm. Even in cancer pearls, significant population at the periphery retains clearly recognized nuclei indicating that cells are still alive, but in the central regions, cells are gradually losing their nuclei on their process of keratinization. I detected a Brm^-, $CD44^-$, MET^-, and $CAV1^-$, and miR-199a$^+$ phenotype in all of the cancer pearls where the cell retained nuclei, which recapitulated that of type 2 cells (Fig. 21 within the broken line). In the area between solid line and the cancer pearl in Fig. 21, where tumor cells assumed intermediate differentiation status, these 4 proteins and miR-199a were weakly

expressed with various extents. At least in these regions, tumor cells might be undergoing changes from the type 1 cells into the type 2 cells through the process of cellular differentiation.

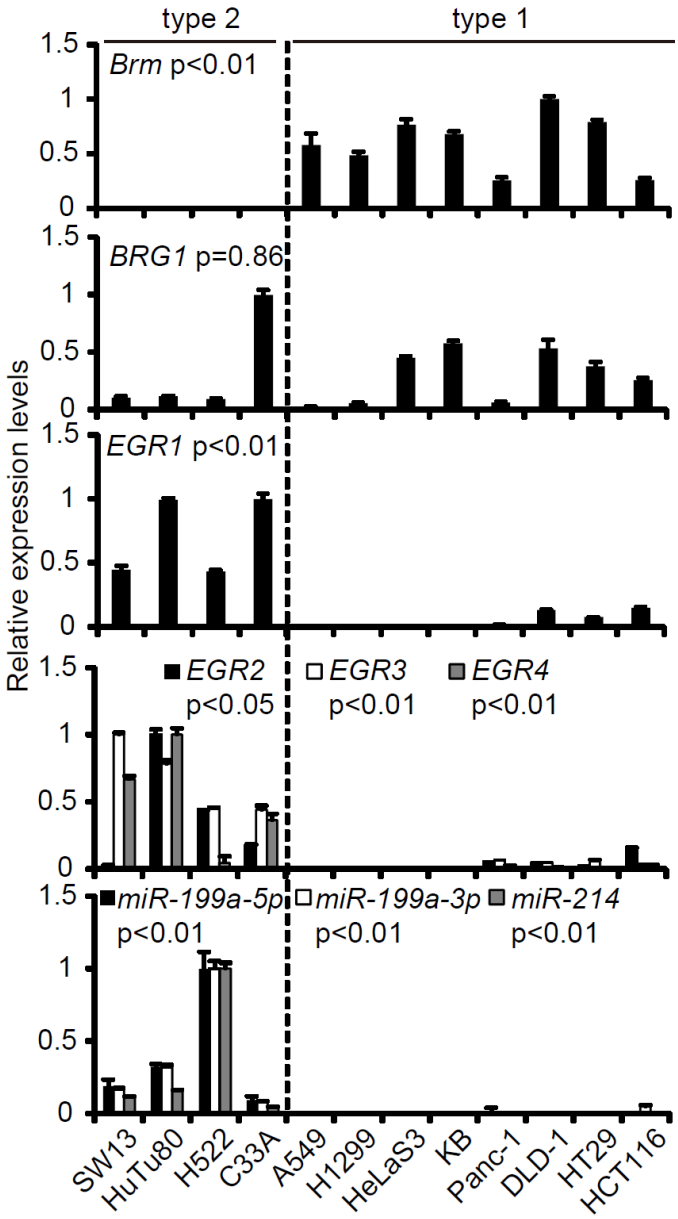

Figure 3. **Basic properties of 12 human cell lines originating from various epithelial tumors.** Relative expression levels of *Brm*, *BRG1*, *EGR1*, *EGR2*, *EGR3*, and *EGR4* mRNA and mature miR-199a-5p, -3p, and miR-214 were determined by quantitative RT-PCR. The relative expression levels are shown by taking the highest levels as 1.0. The data represent the means ± S.D. (n=3). P values were determined using Mann-Whitney test.

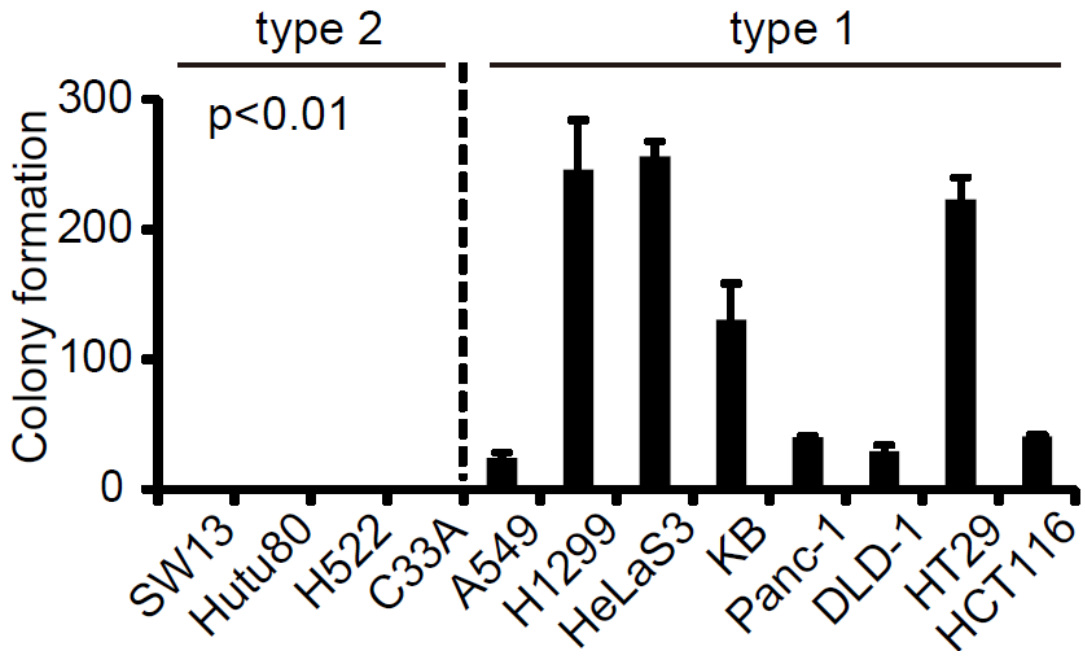

Figure 4. **Numbers of colonies formed in soft agar by each cell line.**
Numbers of colonies (more than 150 μm in diameter) in soft agar were counted 21–28 days after 1,000 cells were seeded in 60 mm plates. The data represent the means ± S.D. (n = 3). P values were determined using Mann-Whitney test.

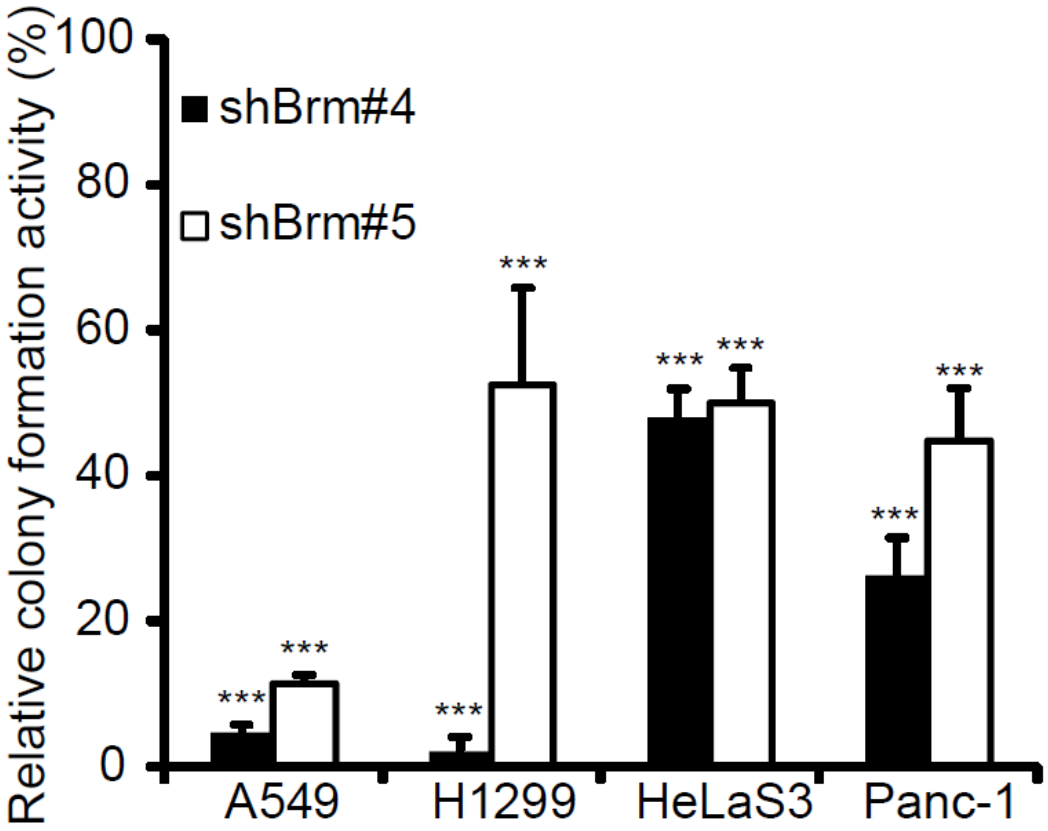

Figure 5. **Brm plays a pivotal role in anchorage-independent growth.**
Four type 1 cell lines transduced with retroviral vectors expressing shBrm (#4 or #5) or shCre#4 (negative control) were seeded as in Figure 4. Colony numbers of shBrm-expressing cells were compared with those of shCre#4-expressing cells and the ratio was shown as a percentage. The data represent the means ± S.D. (n = 4). Asterisks indicate P value, compared with those transduced with shCre#4 . *P<0.05, **P<0.01, ***P<0.001

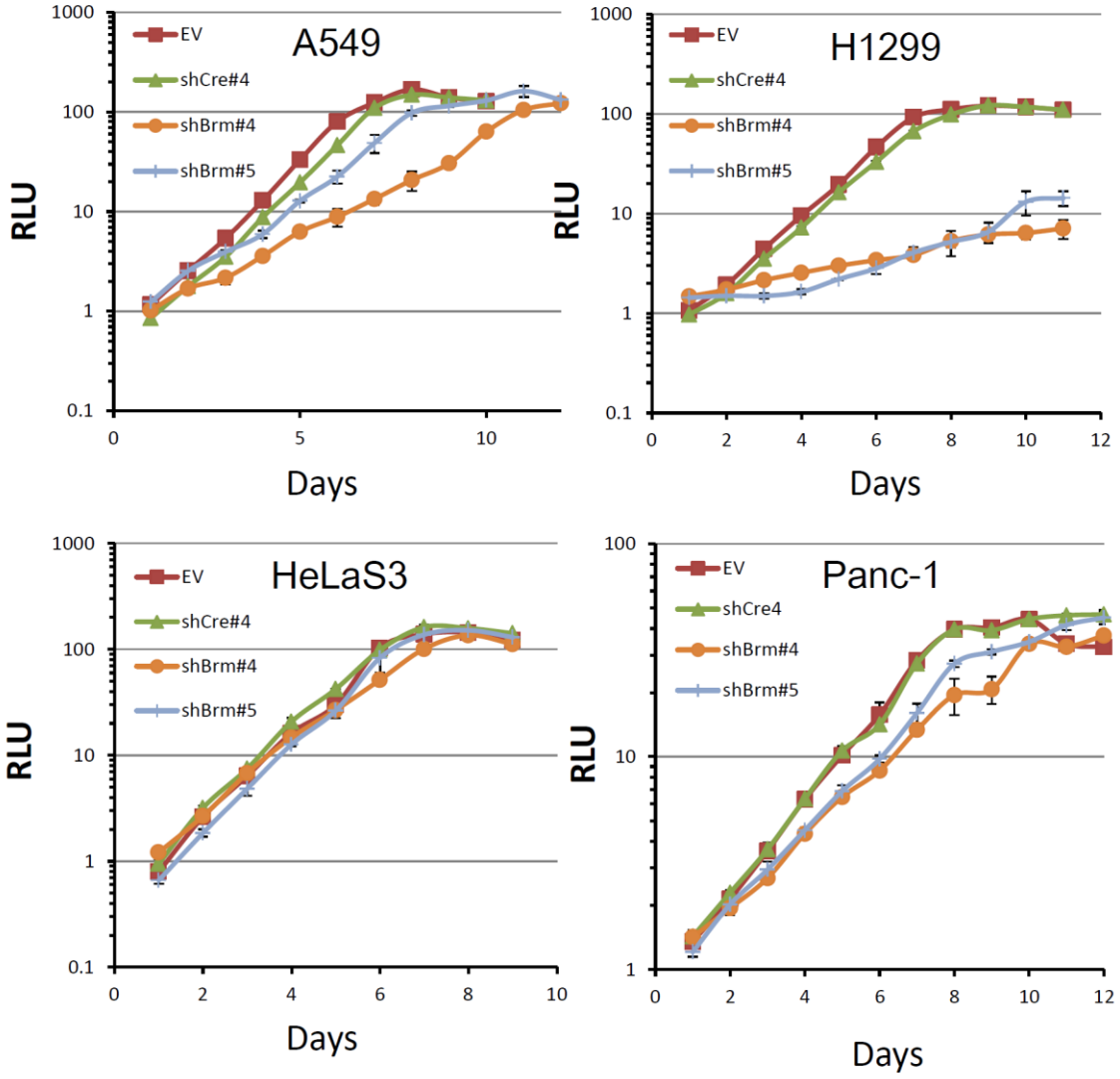

Figure 6. **Growth curve analysis of four type 1 cell lines that were transduced with retroviral vector expressing shBrm (#4 or #5) or shCre#4 (negative control).** Each cell numbers were measured by CellTiter-Glo™ Luminescent Cell Viability Assay (Promega). RLU means relative luciferase units. EV = transduced with empty vector; pSSSP.

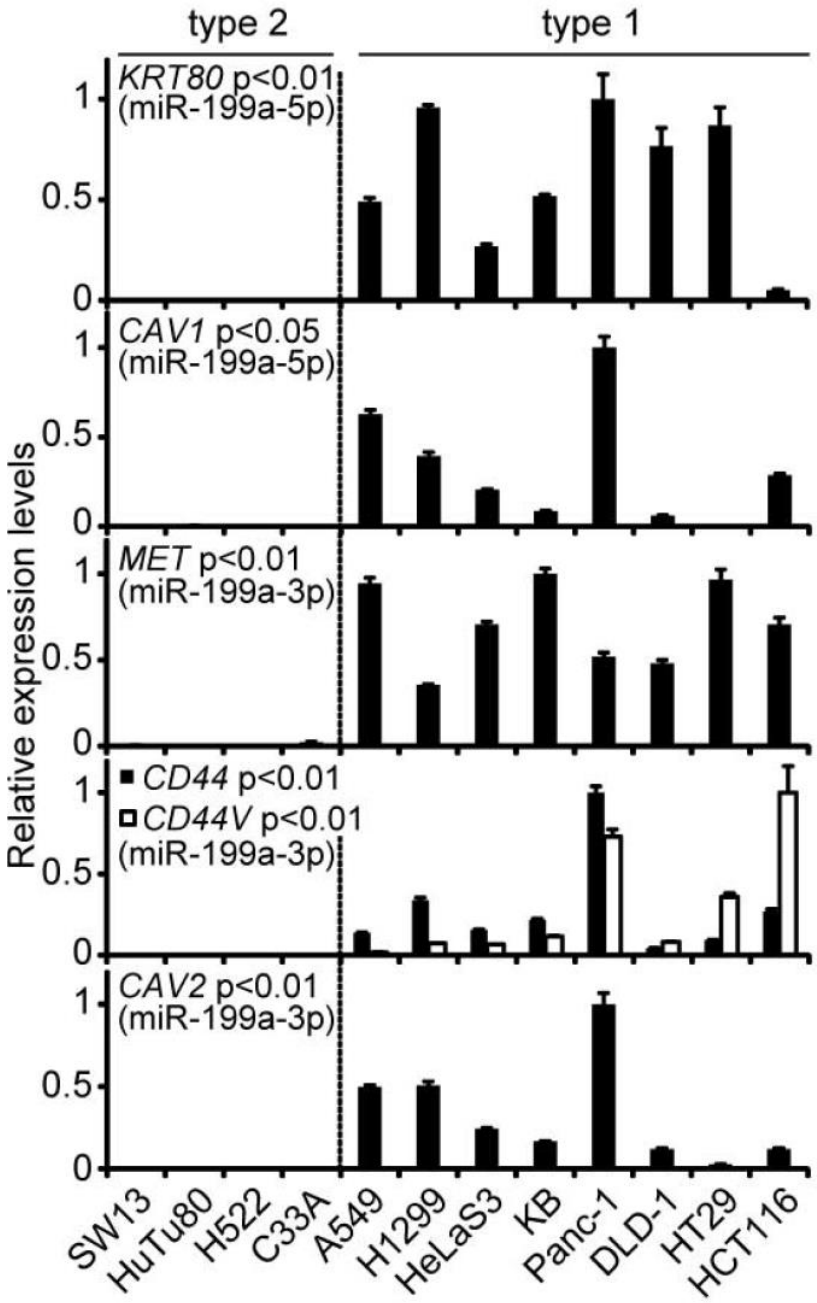

Figure 7. **mRNA expression profiles of each type 1 specific (miR-199a-5p or -3p target) gene in the epithelial tumor cell line panel, as determined by quantitative RT-PCR.** The relative expression levels are shown by taking the highest levels as 1.0. P values were determined using Mann-Whitney test.

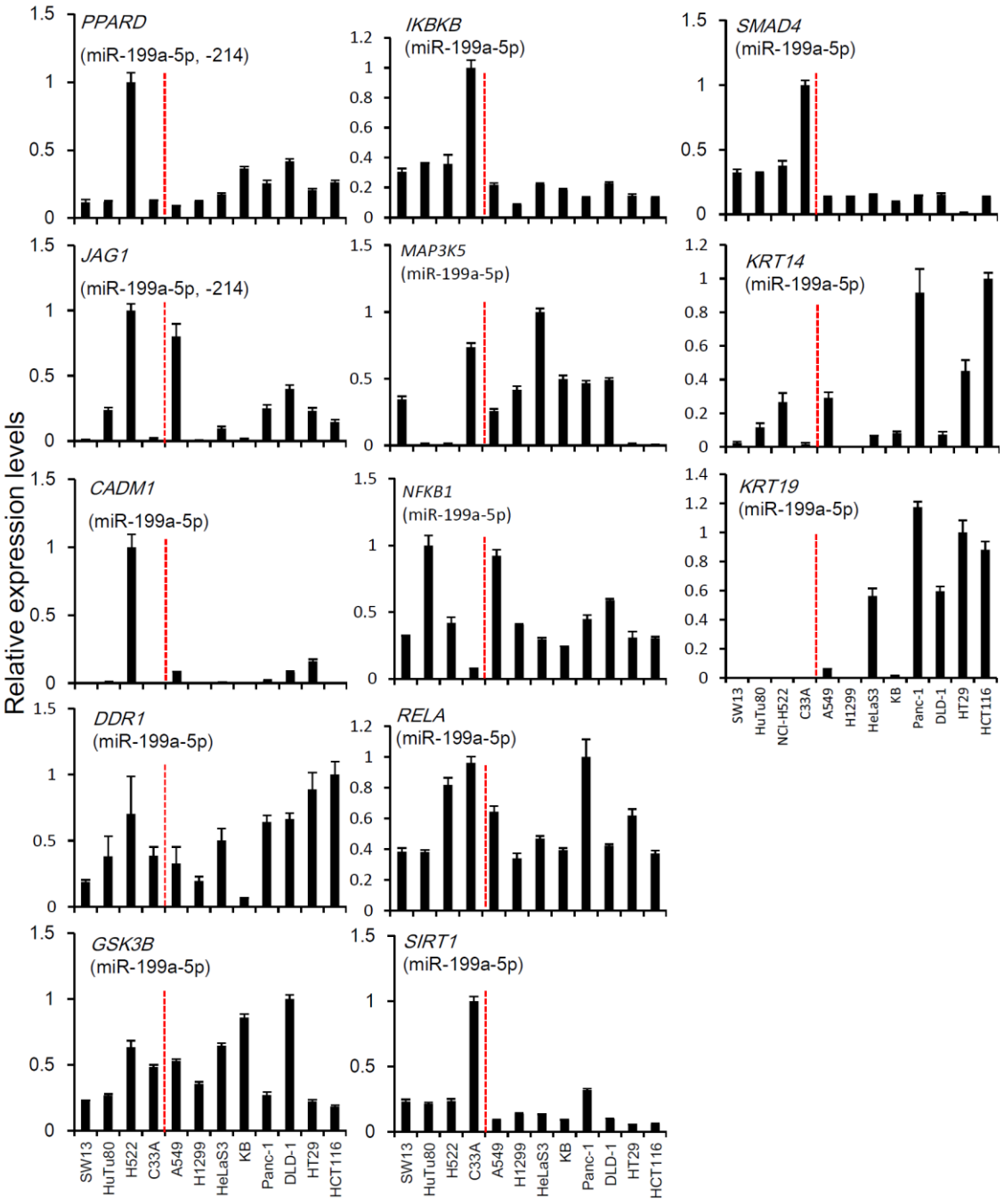

Figure 8. mRNA expression profiles of each miR-199a-5p target gene in the epithelial tumor cell line panel, as determined by quantitative RT-PCR. The relative expression levels are shown by taking the highest levels as 1.0. Red break lines indicate the boundary between type 1 and type 2 cell lines.

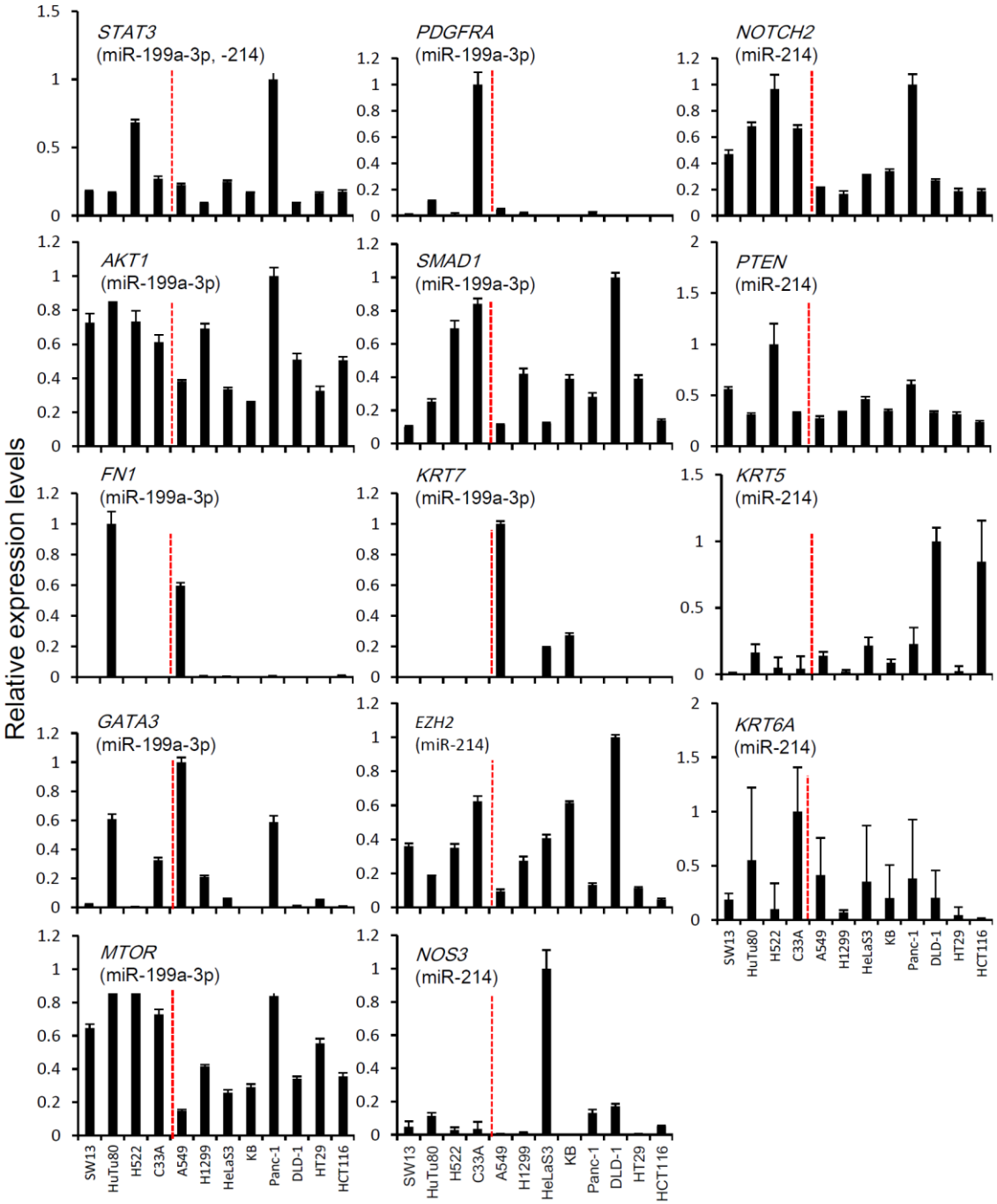

Figure 9. **mRNA expression profiles of each miR-199a-3p, -214 target gene in the epithelial tumor cell line panel, as determined by quantitative RT-PCR.** The relative expression levels are shown by taking the highest levels as 1.0. Red break lines indicate the boundary between type 1 and type 2 cell lines.

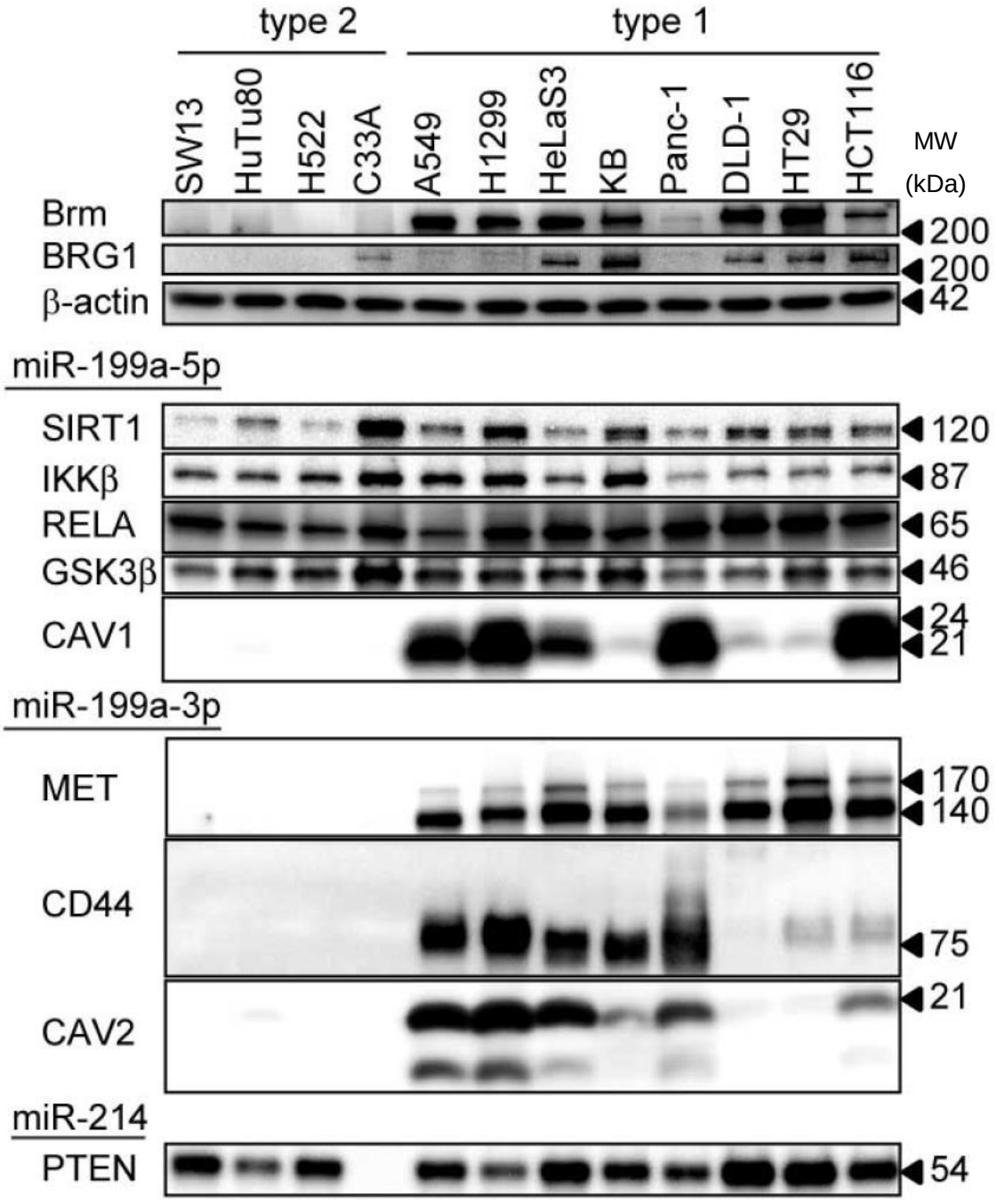

Figure 10. **Protein expression levels of Brm, BRG1, and four type 1-specific genes products as well as five type-independent gene products.** Protein expression levels were analyzed by western blotting using 10 gels. β-actin was used as the loading control for each gel.

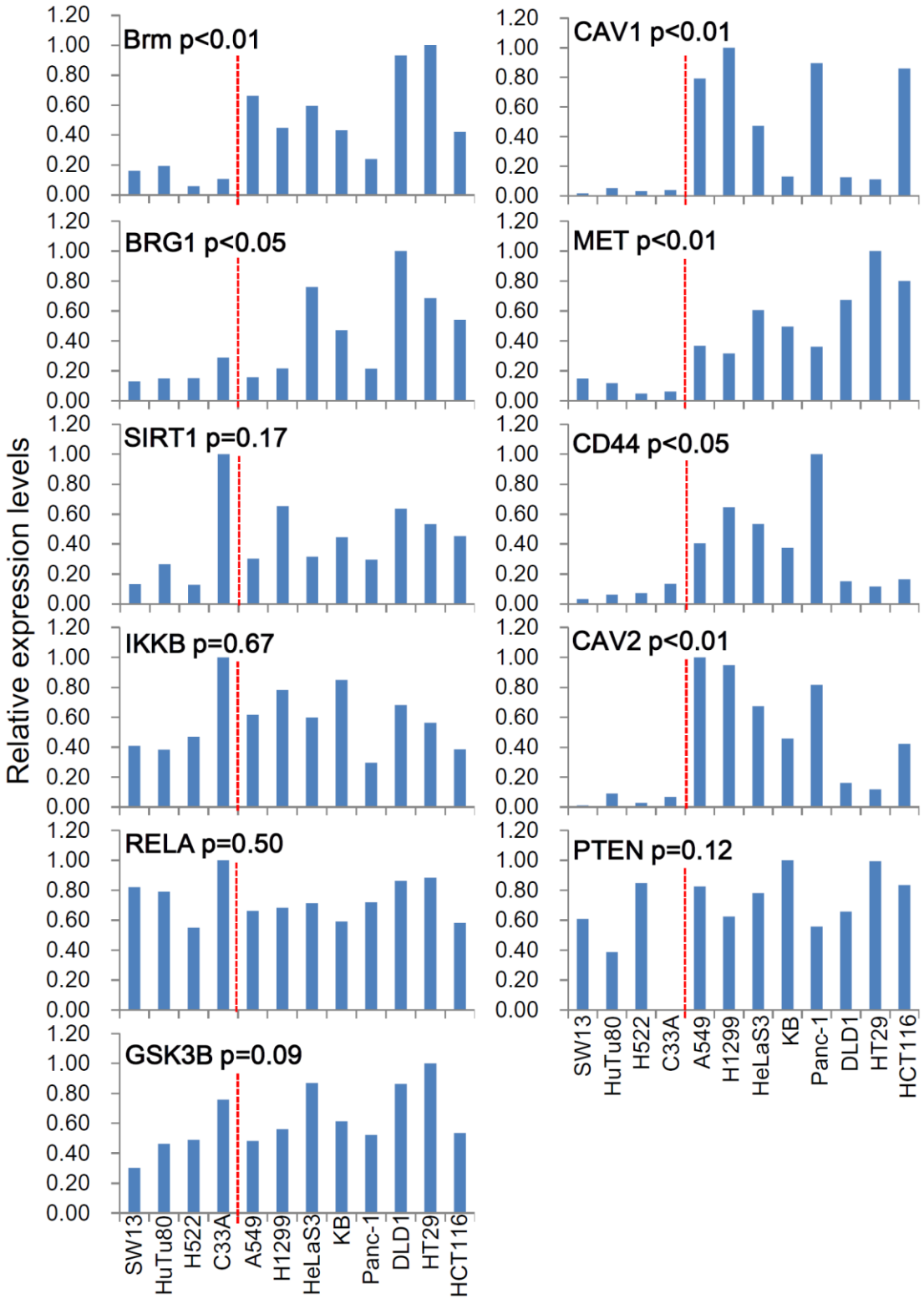

Figure 11. **Protein expression in the epithelial tumor cell line panel, as determined by western blot.** The relative expression levels are shown by taking the highest levels as1.0. Red break lines indicate the boundary between type 1 and type 2 cell lines.

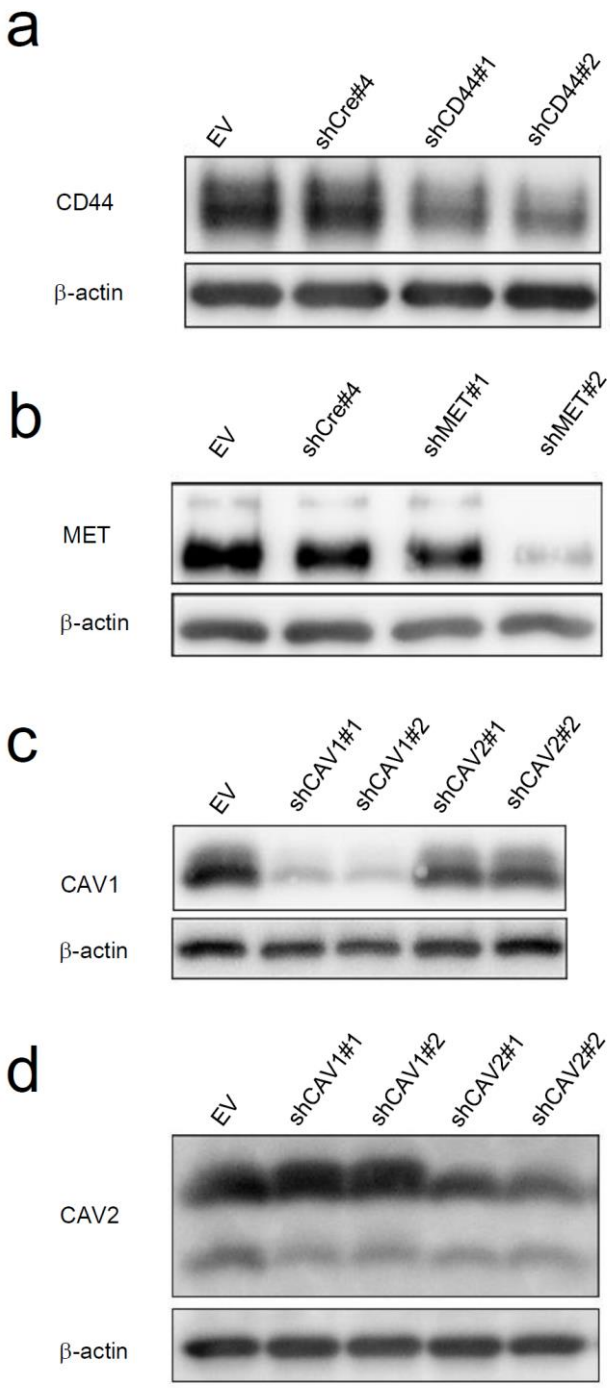

Figure 12. **Knockdown efficiency of shRNAs against CD44, MET, CAV1, and CAV2.** Each efficiency of shRNAs was determined by western blot analysis of A549 cells. Cells were transduced with shRNA-expressing retroviral vectors against CD44 (a), MET (b), CAV1 (c) or CAV2(d), and Cre#4 (negative control), and total proteins were prepared and analyzed by western blotting using the corresponding antibody. EV=transduced with empty vector; pSSSP.

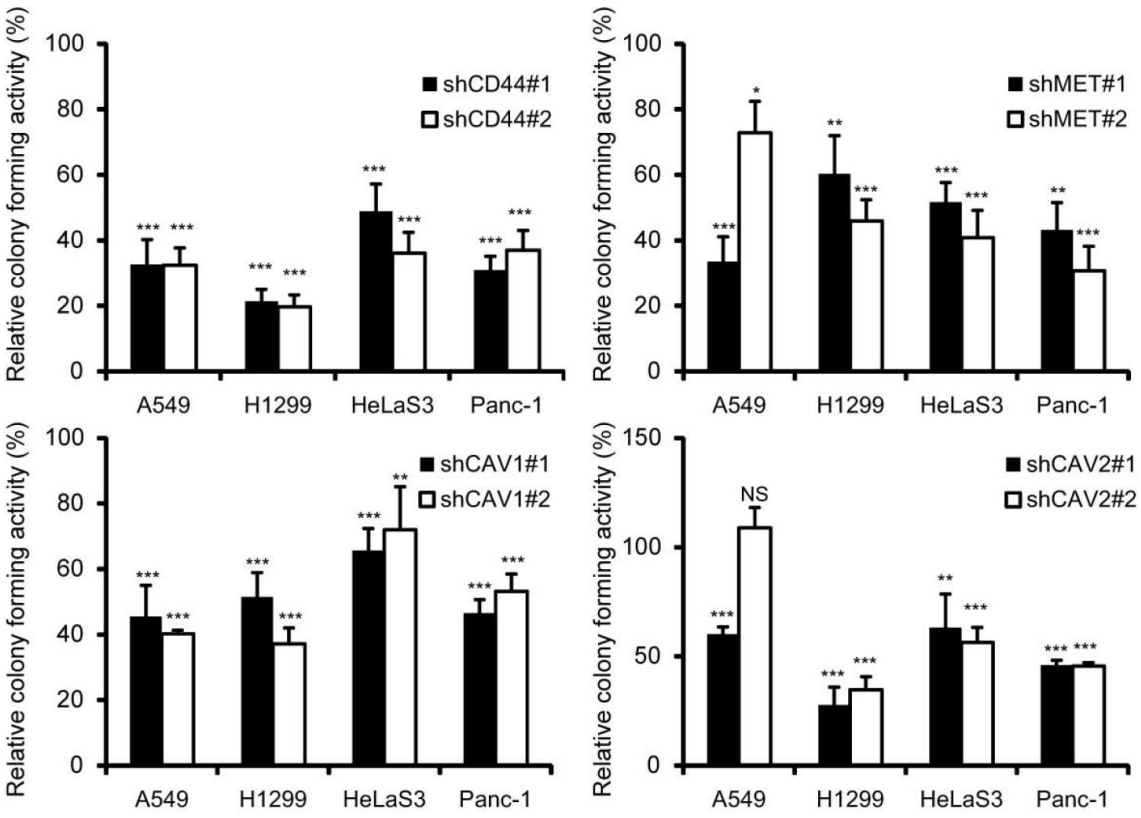

Figure 13. **Effect of single knockdown of several type 1-specific genes on anchorage-independent growth of four type1 cell lines.** 300-1,000 cells of A549, H1299, HeLaS3 and Panc-1 transduced with retrovirus vectors expressing shCD44 (#1 or #2), shMET (#1 or #2), shCAV1 (#1 or #2), shCAV2 (#1 or #2) or sh Cre#4 (a negative control) were seeded in 60mm plates. Colony numbers of these shRNA expressing cells were compared to those of shCre#4 expressing cells and the ratio was shown in percentage. The data represent the means ± S.D. (n = 4). Asterisks indicate P value, compared with those transduced with shCre#4 . NS, not significant. *P<0.05, **P<0.01, ***P<0.001

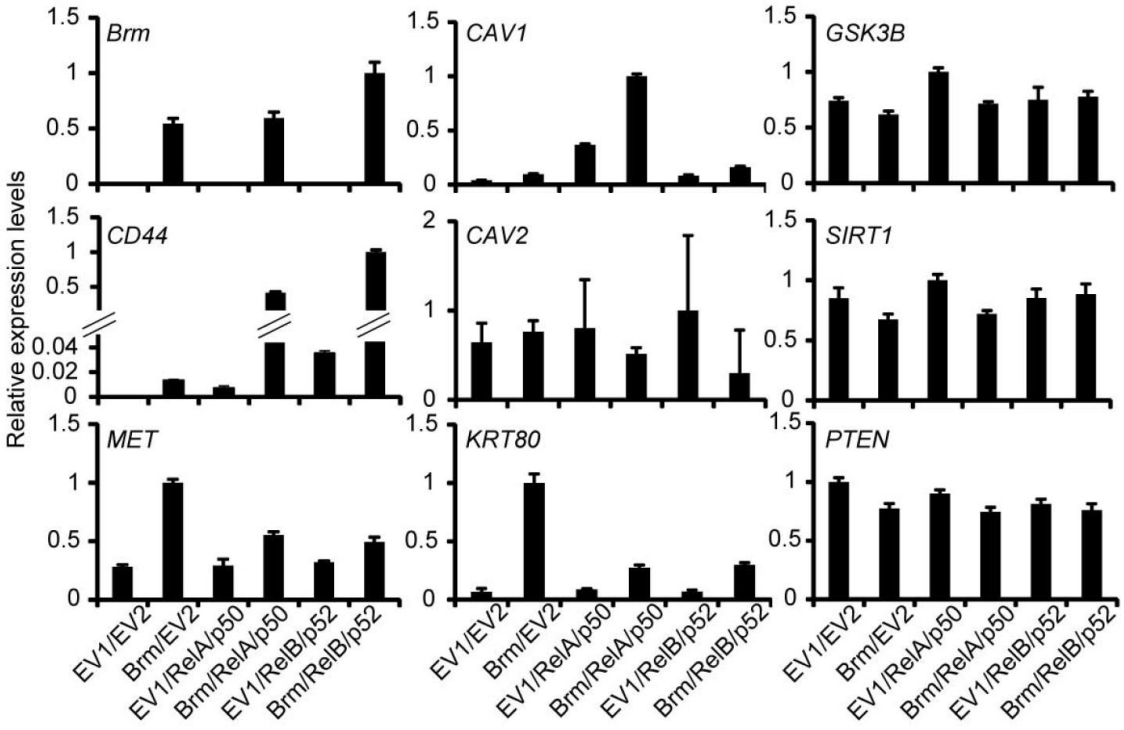

Figure 14. *Brm* is required for the expression of some type 1-specific genes in a type 2 cell line. Expression of *Brm* and type 1-specific (*CD44*, MET, *CAV1*, *CAV2*, and *KRT80*) and non-type-specific (*GSK3β*, *SIRT1* and *PTEN*) genes measured by quantitative RT-PCR in SW13 cells transfected with a Brm expression vector or an empty vector (EV1;pCAG-IG) with or without NFκB dimers (RelA/p50, RelB/p52) or another empty vector (EV2;pRK5). Total RNAs were collected after 48hr of transfection. The highest expression level was taken as 1.0. The data represent the means ± S.D. (n = 3).

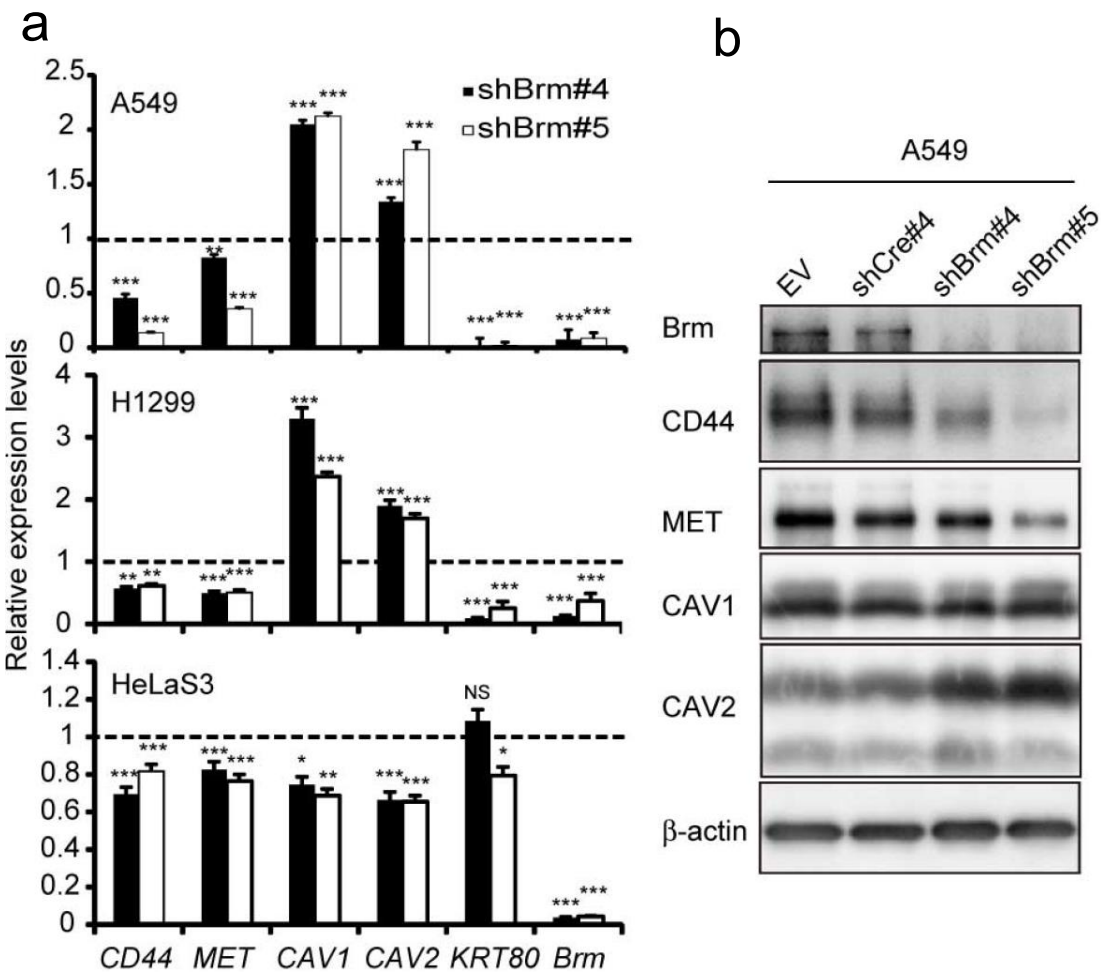

Figure 15. **Effect of knockdown of *Brm* in some type 1 cell lines.** (**a**) Relative expression levels of *CD44* (all transcripts), *MET*, *CAV1*, *CAV2*, and *KRT80* as well as *Brm* mRNA in three cell lines of type 1 cells transduced with shBrm-expressing retroviral vector. The expression levels of cells transduced with shCre#4-expressing vector was taken as 1.0. The data represent the means ± S.D. (n = 3). Asterisks indicate P value, compared with those transduced with shCre#4 . NS, not significant. *P<0.05, **P<0.01, ***P<0.001. (**b**) Protein analysis of the parallel A549 cultures prepared as shown in **(a)**. β-actin was used as the internal control.

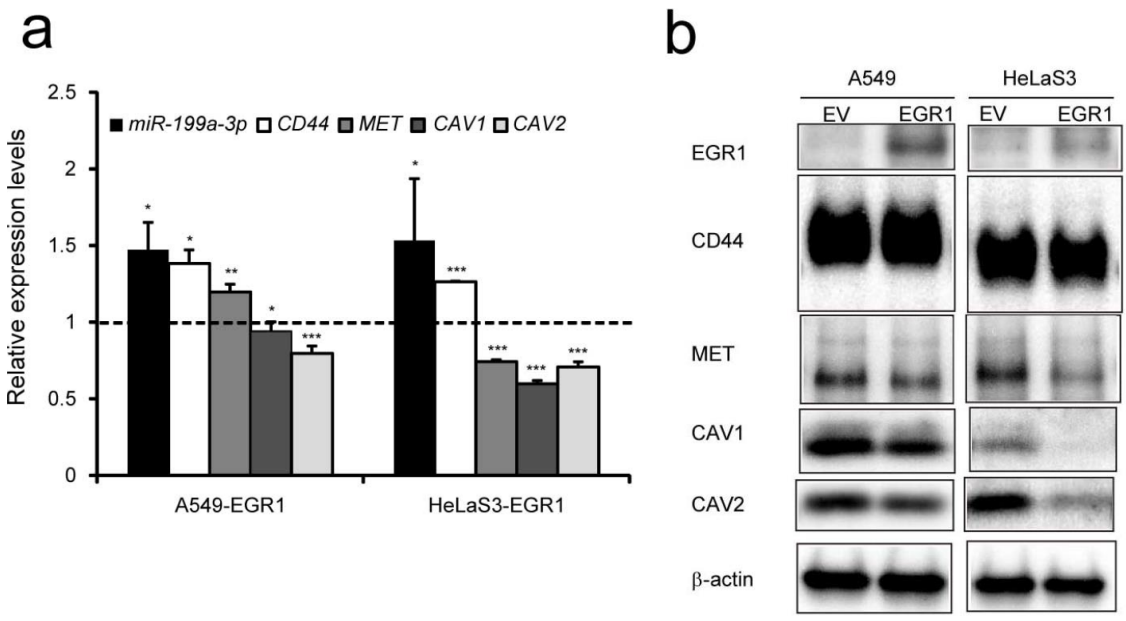

Figure 16. **Effects of exogenous EGR1 expression in type 1 cells.** (**a**) Relative expression levels of miR-199a-3p and type 1-specific mRNAs were determined by quantitative RT-PCR in A549 and HeLaS3 cells which were transduced with retroviral vectors expressing EGR1. The expression levels of cells transduced with empty vector was taken as 1.0. The data represent the means ± S.D. (n = 3). Asterisks indicate P value, compared with those transduced with empty vector. *P<0.05, **P<0.01, ***P<0.001 (**b**) Analysis of type 1-specific gene products and EGR1 in the parallel cultures prepared in **a** by western blotting. β-actin was used as the loading control. The Relative expression levels of each protein including two additional sets of blots were quantified in Table 2.

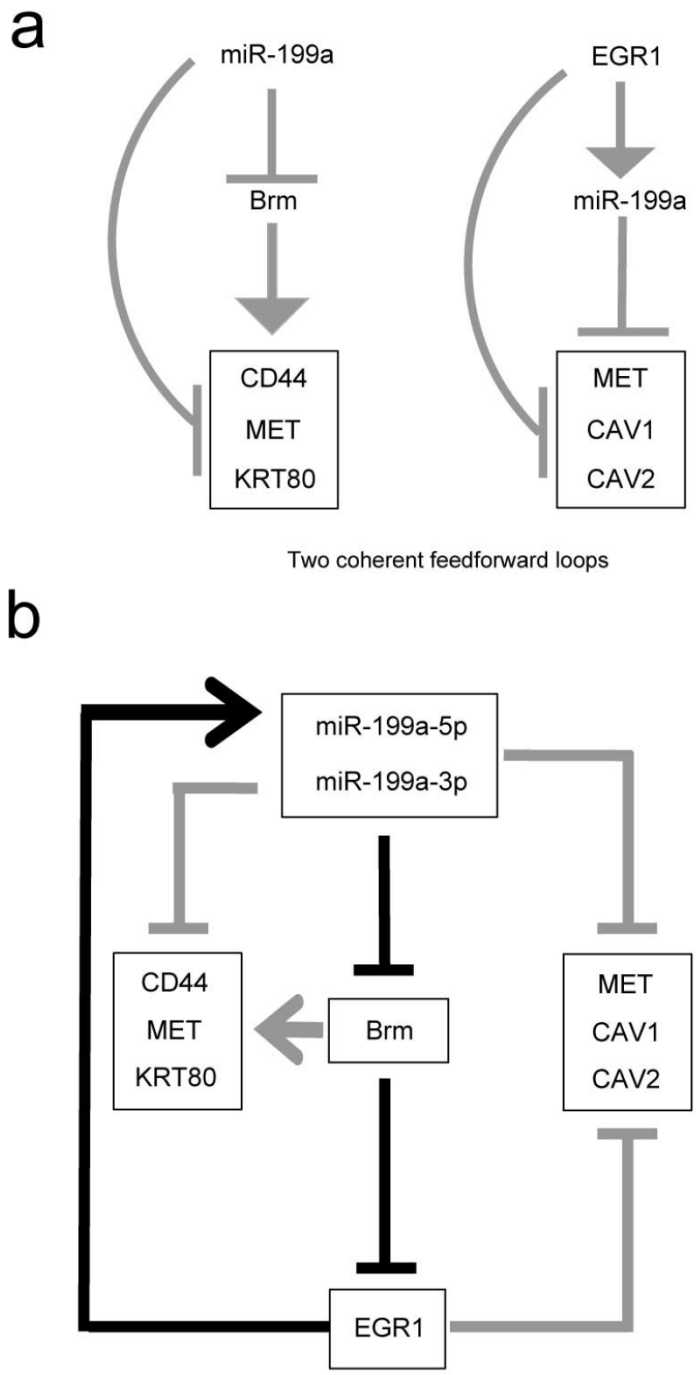

Figure 17. **Models of the regulatory networks operating in various epithelial tumor cell lines.** (**a**) Two feedforward loops that function to establish type 1-specific gene expression in an all-or-none manner. (**b**) A double-negative feedback loop (indicated by black arrows) is integrated by the two feedforward loops (indicated by gray arrows) shown in **a**.

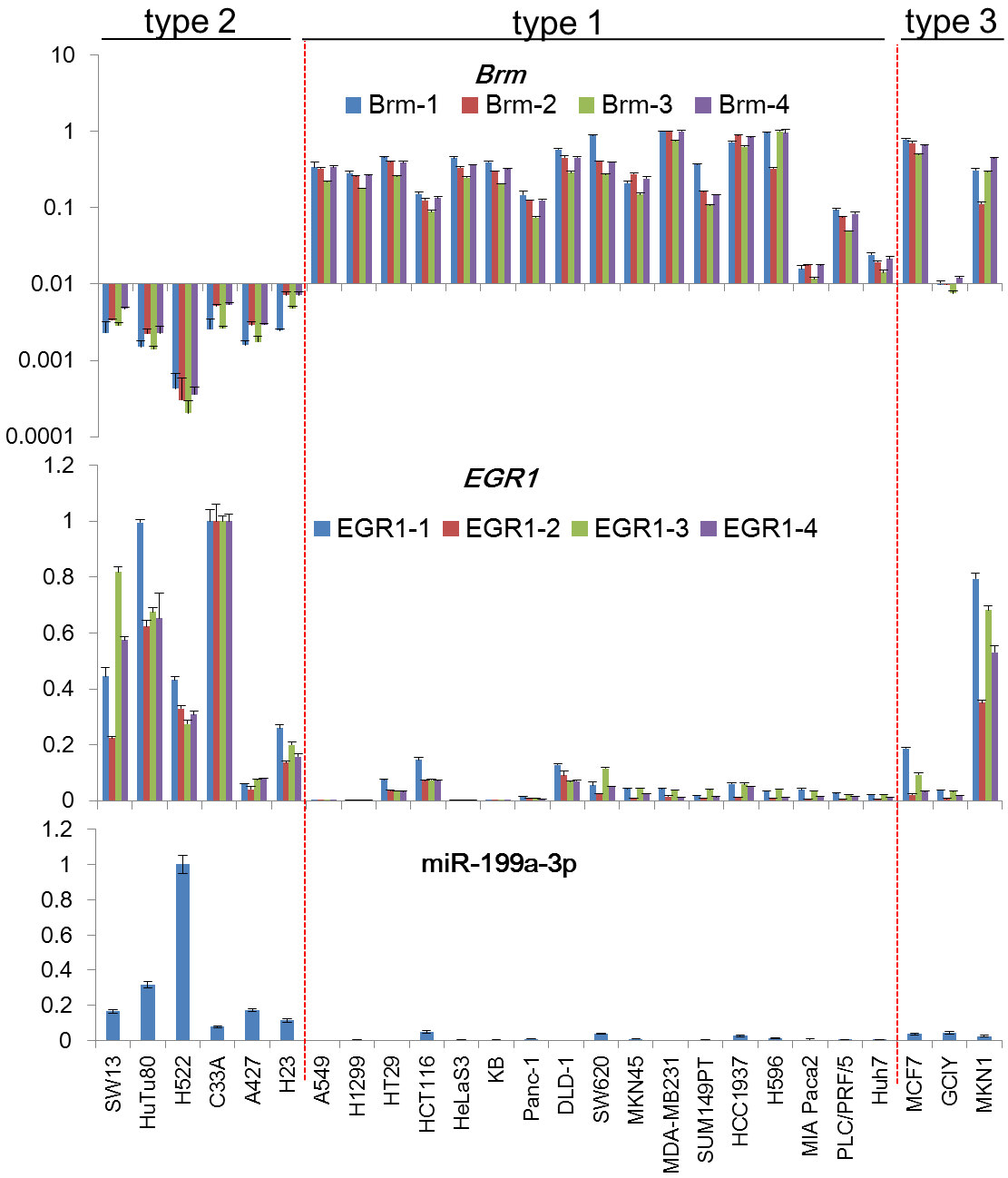

Figure 18. Gene expression analysis on an extended epithelial tumor cell line panel. Expression profiles of *Brm* and *EGR1* mRNA and mature miR-199a-3p RNA of 26 cell lines, as determined by quantitative RT-PCR. Three additional primer pairs were designed and for *Brm* and *EGR1* mRNA quantification other than used in Fig. 3 (Brm-1, EGR1-1). The relative expression levels are shown by taking the highest as 1.0. Two red vertical break lines indicate the boundary among each type cell lines. Detailed criteria for type1-3 cells were indicated in Table 3.

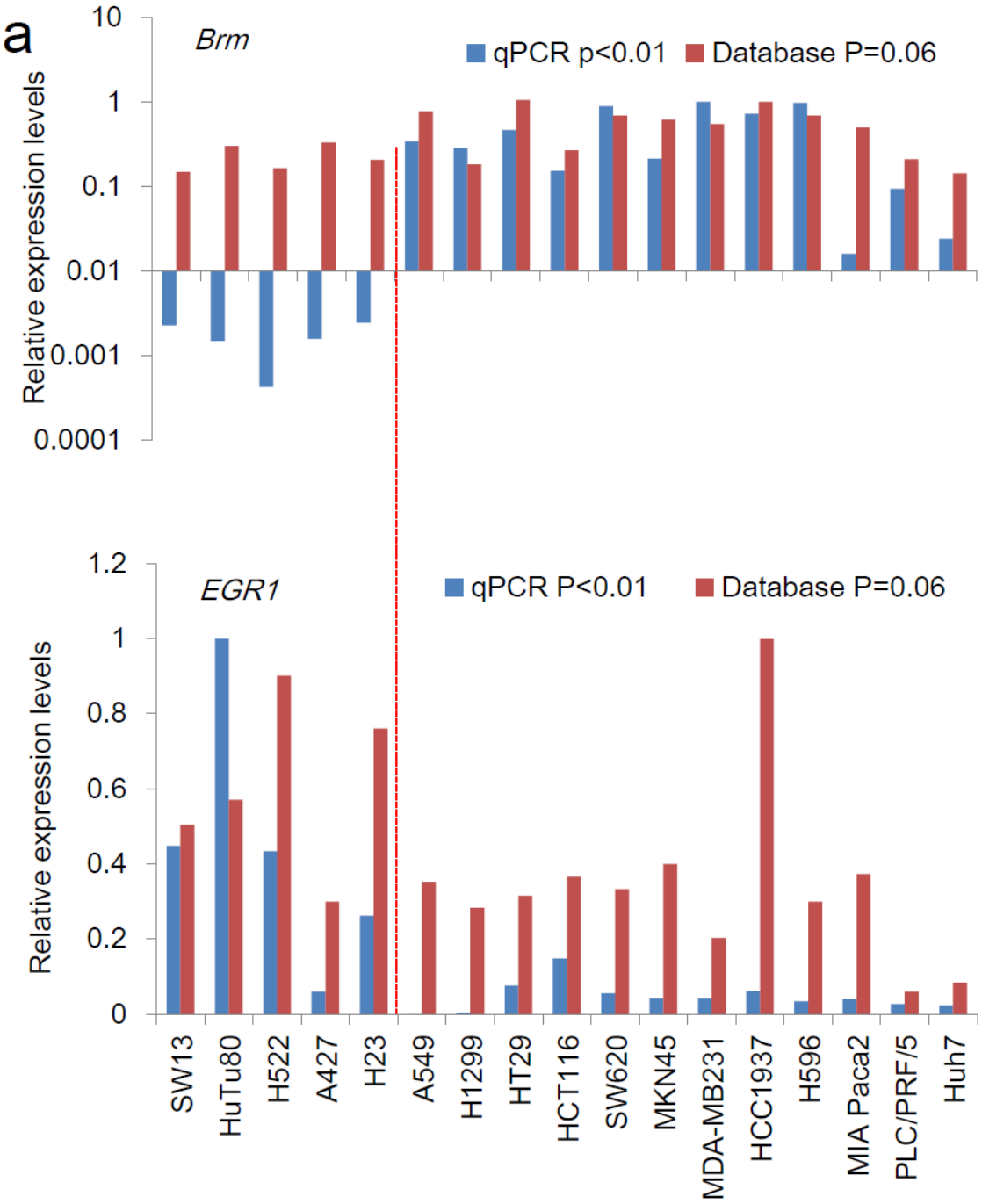

Figure 19. Comparisons of expression profiles of Brm, EGR1, and type 1 specific genes in the epithelial tumor cell line panel between our quantitative RT-PCR (qPCR) data and Sanger Database. The each relative expression levels are shown by taking the highest levels as 1.0. Red break lines indicate the boundary between type 1 and type 2 cell lines. P values were determined using Mann-Whitney test.

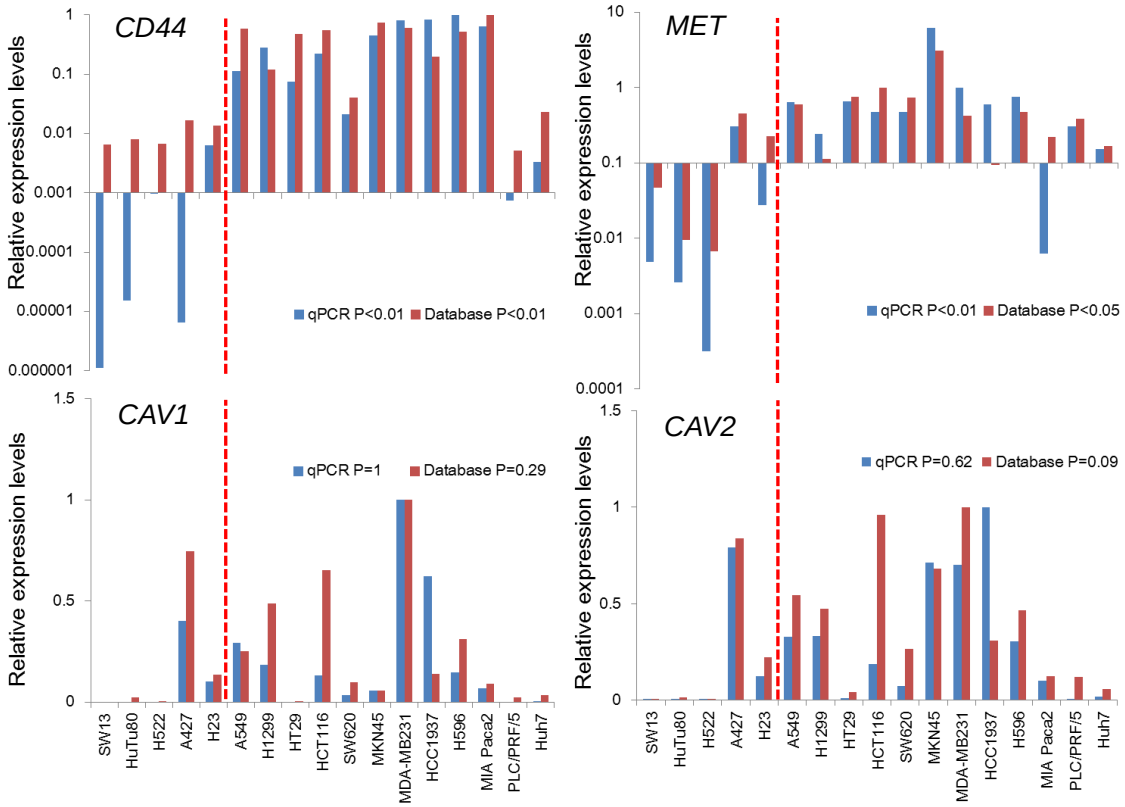

Figure 20. **Expression profiles of *CD44, MET, CAV1 and CAV2* mRNA of 17 cell lines, determined by quantitative RT-PCR (qPCR) (blue bars) or obtained from Sanger database (red bars).** Red break lines indicate the boundary between type 1 and type 2 cell lines. P values were determined using Mann-Whitney test.

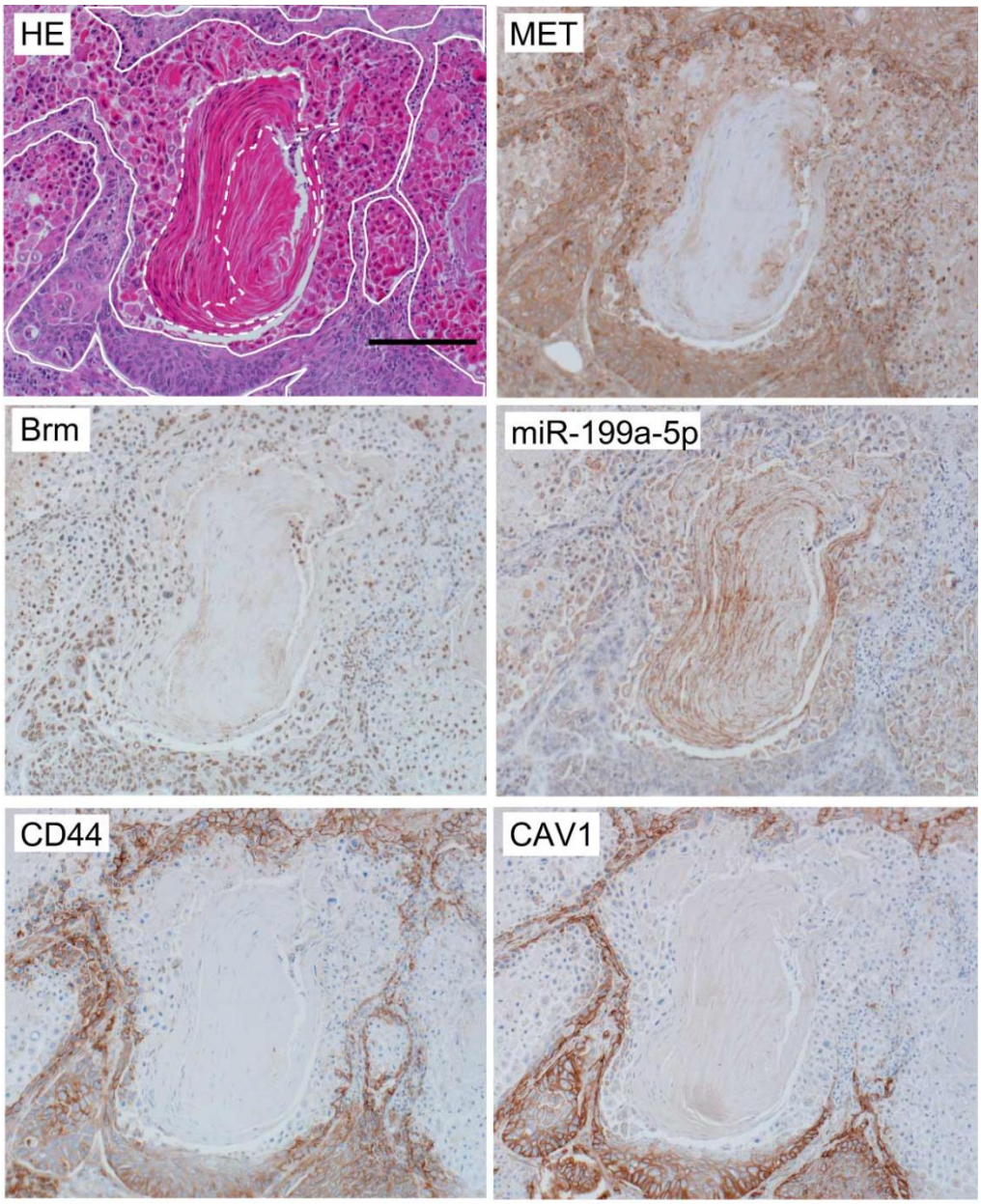

Figure 21. **SCC categorized as NSCLC analyzed by *in situ* hybridization for miR-199a-5p or immunohistochemistry for Brm, CD44, MET, CAV1.** The bar indicates 200 μm. In the HE staining slide, less differentiated cells are surrounded by white solid lines and highly differentiated cells which still retain cellular nuclei at the periphery of a cancer pearl are shown by a white broken line, respectively.

Table 1. List of the examined target genes of miR-199a-5p, -3p and miR-214

Gene	Accession Number	Reported miRNA to target Genes	a	b	c	d	Reference
PPARD	NM_006238	199a-5p, 214	×	×	×	×	Cell Metab 18, 341-54 (2013)
JAG1	NM_000214	199a-5p, 214	○	○	5p:○, 214:x	×	RNA Biol 9, 351-60 (2012)
KRT80	NM_182507	199a-5p, 214	×	×	○	×	-
CADM1	NM_014333	199a-5p	○	×	○	×	J Biol Chem 288, 11845-53 (2013)
DDR1	NM_001954	199a-5p	○	○	○	○	Mol Cancer 9, 227 (2010).
GSK3B	NM_002093	199a-5p	○	○	○	×	Cancer Lett 315, 189-97 (2012)
IKBKB	NM_001556	199a-5p	○	○	○	×	Oncogene 27, 4712-23 (2008)
MAP3K5	NM_005923	199a-5p	○	×	○	×	-
NFKB1	NM_003998	199a-5p	○	×	○	×	Am J Respir Crit Care Med 189, 263-73 (2014)
RELA	NM_021975	199a-5p	×	×	×	×	Am J Respir Crit Care Med 189, 263-73 (2014)
SIRT1	NM_012238	199a-5p	○	○	○	○	Circ Res 104, 879-86 (2009)
SMAD4	NM_005359	199a-5p	×	×	×	○	Nucleic Acids Res 40, 9286-97 (2012)
CAV1	NM_001753	199a-5p	○	○	○	○	PLoS Genet 9, e1003291 (2013)
KRT14	NM_000526	199a-5p	×	×	○	×	-
KRT19	NM_002276	199a-5p	×	×	×	×	Confirmed by our group
STAT3	NM_003150	199a-3p, 214	×	×	3p:×, 214:○	×	Mol Cancer Ther 10, 1337-45 (2011)
AKT1	NM_005163	199a-3p	×	×	×	○	-
FN1	NM_002026	199a-3p	×	○	○	×	-
GATA3	NM_002051	199a-3p	×	○	×	×	-
MTOR	NM_004958	199a-3p	×	×	○	○	Mol Cancer Ther 10, 1337-45 (2011) Cancer Res 70, 5184-93 (2010)
PDGFRA	NM_006206	199a-3p	×	○	○	×	-
SMAD1	NM_005900	199a-3p	×	×	×	×	J Biol Chem 284, 11326-35 (2009)
CAV2	NM_001233	199a-3p	×	○	○	○	J Cell Sci 124, 2826-36 (2011)
CD44	NM_000610	199a-3p	×	×	○	○	Biochem Biophys Res Commun 403, 120-5 (2010) FEBS J 279, 2047-59 (2012)
KRT7	NM_005556	199a-3p	×	×	×	○	Int J Cancer 125, 345-52 (2009)
MET	NM_000245	199a-3p	×	○	×	○	Mol Cancer Ther 10, 1337-45 (2011) Cancer Res 70, 5184-93 (2010)
EZH2	NM_004456	214	×	×	×	○	Mol Cell 36, 61-74 (2009)
NOS3	NM_000603	214	×	×	○	×	Eur J Pharm Sci 38, 370-7 (2009)
NOTCH2	NM_024408	214	×	×	○	×	-
PTEN	NM_000314	214	○	×	○	○	Cancer Res 68, 425-33 (2008)
KRT5	NM_000424	214	○	×	○	×	-
KRT6A	NM_005554	214	×	×	○	×	-

a. mirna.org : (http://www.microrna.org/microrna/home.do), b. PicTar : (http://pictar.mdc-berlin.de/) c. TargetScan : (http://www.targetscan.org/), d. miRTarBase : (http://mirtarbase.mbc.nctu.edu.tw/)

Table 2. **Relative protein expression levels of EGR1, CD44, MET, CAV1 and CAV2 after EGR1 introduction into A-549 or HeLaS3.** Three western blots (one of them was shown in Fig16b) were used for quantification after normalizing with beta-actin (loading control). The protein bands of cells transduced with the empty vector (EV) were taken as 1.0 and P-values were calculated by the student's t-test (n=3).

	A549		HeLaS3	
Protein	Relative expression levels	P value	Relative expression levels	P value
EGR1	2.16±0.62	p<0.001	1.91±0.25	p<0.001
CD44	0.96±0.11	p=0.42	1.06±0.07	p=0.07
MET	075±0.03	p<0.01	0.80±0.11	p<0.05
CAV1	0.77±0.06	p<0.001	0.61±0.12	p<0.001
CAV2	0.76±0.12	p<0.01	0.62±0.13	p<0.001

Table 3. Epithelial tumor cell lines used in this study and their classification.

Cell lines used in Fig. 3 as the original panel are shown in blue. Cell lines that are newly added in Fig. 18 are shown in white. For *Brm* and *EGR1* mRNA, quantitative RT-PCR data using primer pairs Brm-1 and EGR1-1 were used (Fig. 18). The relative expression levels are shown by taking the highest levels as 1.0. Criteria for classification of three expression levels (+, ±, -) are summarized in the upper part.

	Brm	EGR1	miR-199a-3p
+	0.10<	0.15<	0.10≦
±	0.02-0.10	0.06-0.15	-
-	<0.02	<0.06	<0.10

Type	Cell line	Origin	Brm	EGR1	199a-3p
2	SW13	Adrenal carcinoma	0.00	0.45	0.17
2	HuTu80 (AZ521)	Duodenum adenocarcinoma	0.00	0.99	0.32
2	NCI-H522	NSCLC	0.00	0.43	1.00
2	C33A	Cervical carcinoma	0.00	1.00	0.08
2	A427	Lung carcinoma	0.00	0.06	0.17
2	H23	NSCLC	0.00	0.26	0.11
1	A549	Lung carcinoma	0.34	0.00	0.00
1	H1299	NSCLC	0.28	0.00	0.00
1	HT29	Colorectal adenocarcinoma	0.46	0.08	0.00
1	HCT116	Colorectal adenocarcinoma	0.15	0.15	0.05
1	HeLaS3	Cervical carcinoma	0.44	0.00	0.00
1	KB	Cervical carcinoma	0.40	0.00	0.00
1	Panc-1	Pancreatic carcinoma	0.15	0.00	0.01
1	DLD-1	Colorectal adenocarcinoma	0.58	0.13	0.00
1	SW620	Colorectal adenocarcinoma	0.89	0.05	0.04
1	MKN45	Gastric adenocarcinoma	0.21	0.04	0.01
1	MDA-MB231	Mammary adenocarcinoma	1.00	0.04	0.00
1	SUM149PT	Ductal carcinoma	0.37	0.02	0.01
1	HCC1937	Ductal carcinoma	0.72	0.06	0.03
1	H596	Lung adenosquamous carcinoma	0.96	0.03	0.01
1	MIA Paca2	Pancreatic carcinoma	0.02	0.04	0.01
1	PLC/PRF/5	Hepatoma	0.09	0.03	0.01
1	Huh7	Hepatoma	0.02	0.02	0.01
3	MCF7	Mammary adenocarcinoma	0.78	0.19	0.04
3	GCIY	Stomach carcinoma	0.01	0.04	0.04
3	MKN1	Stomach adenosquamous carcinoma	0.31	0.79	0.03

Discussion

Using 12 cell lines that were strictly derived from human epithelial tumors, I confirmed the findings of our previous report that these cells can be classified into type 1 [mir-199a(-) /Brm(+)/EGR1(-)] (8 lines) or type 2 [miR-199a(+)/Brm(-)/EGR1(+)] (4 lines) cells[25]. Furthermore, I was able to efficiently identify the type 1-specific genes by setting the reported miR-199a and miR-214 target genes as the candidates. Some of the identified type 1-specific genes (*CD44*, *MET*, and *KRT80*) required *Brm*, whereas others (*CAV1*, *CAV2* and probably *MET*) required the absence of EGR1 for their efficient expression, indicating that two coherent feedforward loops are formed (Fig. 17a). These two feedforward loops are integrated into the robust double-negative feedback loop forming a regulatory network that functions as an efficient switch that determines the expression levels of these type 1-specific genes in an all-or-none manner (Fig. 17b). Thus, the current situation would be a good example of a network formed by multiple miRNA-mediated feedback and feedforward loops[44, 45], which are commonly present in a wide variety of cell lines.

In this study, I screened the miR-199a or miR-214 target genes as candidates of type 1 specific genes, however, other genes may be also expressed specifically in type 1 or type 2. Actually, our latest database analysis suggested that several other genes are also

expressed specifically in type 1 or type 2 (unpublished data). For example, several epithelial specific keratin genes including keratin-7, -19, and -80 are specifically expressed in type 1 (Figure. 7, 8, and 9). On the other hand, some neural specific genes are expressed in a type 2 specific manner. Interestingly, by pathological analysis, I observed regions whose expression patterns recapitulated those of type 1 or type 2 cells in the some SCC lesion of NSCLC tissues. This result indicated that type 1 specific gene expressions are correlated to high tumorigenicity *in vivo* as well as *in vitro*. Therefore, I speculate that type 1 cell line is more undifferentiated status than type 2, and that switching from type 1 type 2 leads to a novel cancer therapy in SCC. Actually, in acute promyelocytic leukemia, differentiation therapy using all-trans retinoic acids uses for treatments[46]. However, the terminal differentiation mechanisms of keratinization process which are observed in type 2 like cancer lesions are unsolved and necessary to be elucidated. Transition from either type 2 to type 1 or from type 1 to type 2 at this moment is inevitably partial and transient as a practical manner, suggesting that both type 1 and type 2 cells are strongly tied to their own state after the loops are established and therefore stable switching to the opposite type would be also difficult[47, 48]. This robustness of each type may reflect some aspects of "oncogene addiction"[49] or "oncomiR addiction"[50].

Among the type 1-specific genes shown here, *CD44*, *MET*, *CAV1*, and *CAV2* alone significantly contributed to anchorage-independent growth of type 1 cells when tested in knockdown experiments using four type 1 cell lines (Fig. 13). Several previous reports indicated that CD44[511], MET[52], and CAV1[53, 54] are potentially important for colony formation in some epithelial tumor cell lines. I observed that these four genes are all simultaneously suppressed to a marginal level in type 2 cells by the regulatory network shown here, ensuring the anchorage dependency of type 2 cells. Whereas CD44[55, 56], MET[57], CAV1[58], and CAV2[59] have their own multiple downstream signaling pathways, their interplay would also contribute to anchorage-independent growth or metastasis[60, 61]. Importantly, CD44 and MET were reported to co-localize with CAV1 in caveolae[62], and CAV2 is also localized in caveolae when it forms hetero-oligomers with CAV1[63]. In normal epithelial cells, caveolae function as plasma membrane sensors, responding to changes in extracellular matrix via integrin signaling and also as interacting domains with cytoskeltones[39]. By unregulated expression of these four proteins in type 1 cells, their intimate and coordinated interactions would generate strong downstream signaling preferable to grow in soft agar. Therefore, in normal epithelial cells, I expect miR-199a-5p and -3p would fine-tune caveolin function such as homeostasis for plasma membrane integrity, signaling platforms, cytoskeleton remodeling and cell migration.

In addition to overlapping subcellular localizations of these gene products, it should also be pointed out that the genetic loci of *MET*, *CAV1*, and *CAV2* all reside in the fragile chromosomal region, FRA7G at 7q31.2[64]. These regions seems to be neither amplified nor deleted based on the copy number data compiled in CCLE (https://ccle.ucla.edu/); copy number data of eight cell lines (data of SW13, C33A, HeLaS3 and KB are not available) and the copy numbers of this region are distributed from 1.72 to 2.61.

The results in my present study reveal that in normal cells, the interplay between chromatin remodeling factors and miRNAs would fine-tune plasma membrane sensors by several motifs including the miR-199a/Brm/EGR1 axis and two feedforward motifs detected here. These motifs, once misapplied during the process of carcinogenesis, would finally fix the cancer cells to extreme steady states, which cannot be easily reversed. I believe our current findings will give us clues to elucidate how the homeostatic balance is abrogated at cancer initiation to establish type 1 or type 2 tumors and how to guide the development of distinct therapeutic strategies in each case.

Materials and Methods

Cell culture. The following human cell lines were used in this study: SW13 (adrenocortical carcinoma) [SW13(vim-) was used as a subtype of SW13 that is deficient in Brm and BRG1][18]; HuTu80 (duodenum carcinoma; the previous nomenclature, AZ521, was corrected according to the instructions of the American Type Culture Collection); NCI-H522, A549, and NCI-H1299 (non-small cell lung carcinoma); C33A and HeLaS3 (cervical carcinoma); KB (recently shown to be a derivative of HeLaS3); Panc-1 (pancreatic carcinoma); and DLD-1, HT29, and HCT116 (colon carcinoma). All cultures were maintained in Dulbecco's modified Eagle's medium (DMEM) containing 10% fetal calf serum (FCS). A549, NCI-H522, NCI-H1299, C33A, A549, KB, Panc-1, DLD-1, HT29, and HCT116 cell lines were purchased from the American Type Culture Collection. AZ521 (HuTu80) and HeLaS3 cell lines were obtained from the Cell Resource Center for Biomedical Research, Institute of Development, Aging and Cancer, Tohoku University, Japan.

Expression vectors. Expression vectors for Brm (pCAG-Brm-IG)[65] and NF-κB-expressing vectors (pRK5-RelA, -RelB, -p50, and p52)[12] used in this study have been described previously. To generate EGR1 expressing retrovirus vector, a

*Eco*RI-*Not*I DNA fragment of pCMV-SPORT6-EGR1[25] was inserted to the corresponding cloning site of pMXs-IRES-Puro or -Bla.

Plasmid preparation for retroviral vectors expressing shRNA. Pairs of oligonucleotides encoding gene-specific shRNA were synthesized (Table 4) and inserted between the *Bbs*I/*EcoR*I sites of pmU6. The pmU6 derivatives shCre#4[59] [used as negative control (NC)] and shBrm#4[66] were previously described. These pmU6-based plasmids were digested with *Bam*HI and *Eco*RI and inserted between these sites in pSSSP for the retroviral vectors.

DNA transfection and preparation of retrovirus. For the transfection of plasmid vectors into cell lines, Lipofectamine 2000 (Invitrogen Corp.) was used in accordance with the manufacturer's instructions. The preparation and transduction of vesicular stomatitis virus-G (VSV-G) pseudotyped retroviral vectors were performed as described previously[12].

Quantitative RT-PCR. Total RNA was extracted using a mirVana microRNA Isolation Kit (Ambion). To detect coding gene mRNAs, cDNA was synthesized with a

PrimeScript™ RT Reagent Kit with gDNA Eraser (Perfect Real Time) (TaKaRa Bio) in accordance with the manufacturer's instructions. Quantitative (real-time) RT-PCR was performed using a SYBR® Select Master Mix (Applied Biosystems). *GAPDH* was used as an internal control. The primer pairs used are listed in Table 4. For the detection of miRNA, miRNA-specific looped RT-primers and TaqMan probes were used as described by the manufacturer's protocol (Applied Biosystems). *RNUB6* RNA was used as an internal control. PCRs were performed in triplicate using a 7300 Real-Time PCR system (Applied Biosystems).

Western blotting. Total protein extracts were prepared by boiling the cells in SDS sample buffer for 5 min at 95 °C. The proteins were then separated by 10% SDS-PAGE and transferred onto Immobilon-P PVDF membranes (Millipore). Immunoblotting was performed by incubating the membrane overnight at 4 °C with primary antibodies against the following proteins: Brm (ab15597; Abcam), BRG1 (sc-10768; Santa Cruz), EGR1 (#4153; Cell Signaling), CD44 (#3570; Cell Signaling), MET (#8198; Cell Signaling), CAV1(#3267; Cell Signaling), CAV2 (#8522; Cell Signaling), SIRT1 (sc-74465; Santa Cruz), GSK3β (#12456; Cell Signaling), RELA (ab7971; Abcam), PTEN (#9552; Cell Signaling), IKKβ (#8943; Cell Signaling), and β-actin (sc-47778;

Santa Cruz). After three washes with Tris-buffered saline (TBS) containing Tween 20, the membranes were incubated with secondary antibodies [donkey anti-rabbit-horseradish peroxidase (AP182P) and donkey anti-mouse-horseradish peroxidase (AP192P)]; Millipore) for 1 h at room temperature. Signals were detected using ECL reagent (Promega) or ImmunoStar LD (Wako). Amounts of charged protein samples were roughly normalized to β-actin. Relative protein amounts were quantified by Ez-Capture MG (ATTO) using Multi Gauge V3.2 (Fuji Film) software after strict normalization by the internal control, β-actin.

Immunohistochemical staining. Deparaffinization, endogenous peroxidase inactivation, and antigen retrieval of formalin-fixed, paraffin-embedded clinical tissues and immunostaining of Brm were performed as described previously[25, 67]. For CD44 (#3570; Cell Signaling), MET (ab51067; Abcam), and CAV1 (sc-894; Santa Cruz) immunostaining, the sections were incubated overnight at room temperature with the corresponding antibody used for western blotting and washed in phosphate-buffered saline. N-Histofine® Simple Stain™ MAX PO (MULTI) (414154F; Nichirei Biosciences Inc.) were then applied to the slides for 30 min at room temperature, followed by three washes in PBS. The reaction products were visualized using a 50

mg/dL 3,3′-diaminobenzidine tetrahydrochloride solution containing 0.003% H_2O_2. The immunostained sections were evaluated independently by two pathologists in conjunction with hematoxylin and eosin-stained sections from the same lesions.

***In situ* hybridization.** *In situ* hybridization analysis to detect miR-199a-5p in formalin-fixed, paraffin-embedded sections was performed using LNA-modified oligonucleotide probes as described previously[25, 67]. Use of the clinical tissue sections in this study was approved by the Fujita Health University ethical review board for human investigation.

Statistical analysis. Results are presented as means ±S.D. Statistical significance for quantitative RT-PCR assays was determined using a two-tailed Student's t-test. Statistical significance for the differences of a parameter between type 1 and type 2 cell lines was determined using Mann-Whitney test. In both cases, P-values<0.05 were considered statistically significant.

Table 4. List of primer pairs used for quantitative RT-PCR and oligonucleotides used for shRNA expression vector construction.

Gene	F	R	*Gene*	F	R
KRT80	tcagctgaagaaggacctgg	caactccacgaagctctcca	*CD44v*	tctttcaatgacaacgcagca	ttgggtctcttcttccacctg
CADM1	cgtgacagtgatcgagggag	tttcctgtgggggatcggta	*KRT7*	aatgagtttgtggtgctgaagaag	gtcaactccgtctcattgaggg
DDR1	gctggaaggaccgctgg	agtcgggcaaccatgggg	*MET*	atgtgagatgtctccagcatttt	gcaaagctgtggtaaactctgtt
GSK3B	tagtcgagccaaacagacgc	tccaacaagaggttctgcgg	*EZH2*	ctgcttcctacatcgtaagtgc	tgagagcagcagcaaactcc
IKBKB	agactcagatctccccacgg	ctgctgagacatggaagcca	*NOS3*	gagtatgacgtggtgtccctc	tccatcagggcagctgcaaa
MAP3K5	accgggacataaagggtgaca	tatgccagcaagcctctttga	*NOTCH2*	agcactcaggtgtctgcatc	ttctggcagggctgattctg
NFKB1	ttctggaccgcttgggtaac	aatggcattcagaccgtccc	*PTEN*	agtggcggaacttgcaatcctca	tcccgtcgtgtgggtcctgaa
RELA	cctcctgttgtctcgaaccc	tgcctttgcttcccaatcg	*KRT5*	tggagggcgaggaatgcag	catatccagaggaaacactgcttg
SIRT1	tcagtgtcatggttcctttgc	gttcatcagctgggcaccta	*KRT6A*	ttggtaaagcccagcccttcc	agcaggactaggaatcaggctc
SMAD4	ctggcctgttcacaatgagc	tgtgcaaccttgctctctca	*Brm-1*	acaaagggaaaggcaagaaaag	gtcccacttccttctgactgtt
CAV1	cgcgaccctaaacacctcaa	gccgtcaaaactgtgtgtcc	*Brm-2*	taagagtgcccggcagaaaa	gagcttaattttcaccttgactga
KRT14	aggagatcgccacctaccg	cacatctctggatgactgcga	*Brm-3*	cagggcgacagctcagtgaa	ggctccggtacttatgattacga
KRT19	gcgactacagccactactacac	aatcctggagttctcaatggtg	*Brm-4*	tgaccaaatgggcctcaaaga	aaccaggcacaatcaaaccg
STAT3	cccttggattgagagtcaaga	aagcggctatactgctggtc	*EGR4*	tcttcaacctcatgtcgggc	gatccggggagtaaaggtcc
AKT1	ggcaaggtgatcctggtgaa	ggtcgtgggtctggaaagag	*BRG1*	gagtgacgatgacagtgaggag	atgccatctcagctctggac
FN1	agtggaagtgtgagaggcac	tgaggctgcggttggtaaac	*EGR1-1*	agcagcagcagcaccttc	tctcgttgttcagagagatgtca
GATA3	ctcttcgctacccaggtgac	acgactctgcaattctgcga	*EGR1-2*	ccttcaaccctcaggcggac	agcggccagtataggtgatg
MTOR	caggctggctcttgctcata	ggtcacctgagggtgaactg	*EGR1-3*	ctacgagcacctgaccgc	agtggtttggctggggtaac
PDGFRA	gtctggagcgtttgggaaggt	gatctggccgtgggttttagc	*EGR1-4*	gggacatgctcacctctagc	tctggagaaccgaagctcag
SMAD1	cacccgtttcctcactctcc	aaccgcctgaacatctcctc	*EGR2*	ctttgaccagatgaacggagt	gtctggtttctaggtgcagagac
CAV2	ctcgcatctcaagctgggct	tgaaggcagaaccattaggca	*EGR3*	agagaaatgcctcggatgcc	agatcaaactgccctgaggc
CD44	tggcgcagatcgatttgaata	ccgtccgagagatgctgtag	*EGR4*	tcttcaacctcatgtcgggc	gatccggggagtaaaggtcc

shRNA	sense	antisense
Brm#5	tttgaagaaatgtggataaagatcgcttcctgtcacgatctttatccacatttcttctttttg	aattcaaaaaagaagaaatgtggataaagatcgtgacaggaagcgatctttatccacatttctt
CD44#1	tttgaggaaacatttgacttatctgcttcctgtcacagataagtcaaatgtttcctctttttg	aattcaaaaaagaggaaacatttgacttatctgtgacaggaagcagataagtcaaatgtttcct
CD44#2	tttgcccattgttcattcttgtgcgcttcctgtcacgcacaagaatgaacaatgggctttttg	aattcaaaaaagcccattgttcattcttgtgcgtgacaggaagcgcacaagaatgaacaatggg
MET#1	tttgccactcatttagaattctaggcttcctgtcacctagaattctaaatgagtggctttttg	aattcaaaaaagccactcatttagaattctaggtgacaggaagcctagaattctaaatgagtgg
MET#2	tttgtaatttgttgataaatatttgcttcctgtcacaaatatttatcaacaaattacttttttg	aattcaaaaaagtaatttgttgataaatatttgtgacaggaagcaaatatttatcaacaaatta
CAV1#1	tttggtaatttgagagaaatatgagcttcctgtcactcatatttctctcaaattacctttttg	aattcaaaaaaggtaatttgagagaaatatgagtgacaggaagctcatatttctctcaaattac
CAV1#2	tttggaataagttcaaattcttctgcttcctgtcacagaagaatttgaacttattccttttttg	aattcaaaaaaggaataagttcaaattcttctgtgacaggaagcagaagaatttgaacttattc
CAV2#1	tttgctttagtacaatagtatacagcttcctgtcactgtatactattgtactaaagctttttg	aattcaaaaaagctttagtacaatagtatacagtgacaggaagctgtatactattgtactaaag
CAV2#2	tttgctaataagtgacaaataagagcttcctgtcactcttatttgtcacttattagctttttg	aattcaaaaaagctaataagtgacaaataagagtgacaggaagctcttatttgtcacttattag

Acknowledgements

I would like to express the deepest appreciation to my supervisor, Professor Hideo Iba (Division of Host-Parasite Interaction, Institute of Medical Science, the University of Tokyo) for his guidance during my doctoral course. And I thank all the members in our laboratory for their advice. Especially, I appreciate Hiroaki Hiramatsu, Shinya Nakamura, and Kyosuke Kobayashi, who are the members in our laboratory for their help laboratory experiments.

I would like to express great thanks to Dr. Ken-Ichi Inada and Dr. Kazuya Shiogama (1st Department of Pathology, Fujita Health University School of Medicine) for their help on Immunohistochemical staining and in situ hybridization analysis, Dr. Seiya Imoto (Laboratory of DNA Information Analysis, Human Genome Center, Institute of Medical Science, The University of Tokyo) for Database analysis and statistical analysis. I am also very grateful to Yoshida Scholarship Foundation for financial support.

Finally, my most sincere acknowledgements are toward all my family for their encouragements.

Refurences

1. Wilson, B.G. & Roberts, C.W. SWI/SNF nucleosome remodellers and cancer. *Nat Rev Cancer* **11**, 481-92 (2011).

2. Ebert, M.S. & Sharp, P.A. Roles for microRNAs in conferring robustness to biological processes. *Cell* **149**, 515-24 (2012).

3. Iliopoulos, D., Hirsch, H.A. & Struhl, K. An epigenetic switch involving NF-kappaB, Lin28, Let-7 MicroRNA, and IL6 links inflammation to cell transformation. *Cell* **139**, 693-706 (2009).

4. Gurtan, A.M. & Sharp, P.A. The role of miRNAs in regulating gene expression networks. *J Mol Biol* **425**, 3582-600 (2013).

5. Yaniv, M. Chromatin remodeling: from transcription to cancer. *Cancer Genet* **207**, 352-357 (2014).

6. Khavari, P.A., Peterson, C.L., Tamkun, J.W., Mendel, D.B. & Crabtree, G.R. BRG1 contains a conserved domain of the SWI2/SNF2 family necessary for normal mitotic growth and transcription. *Nature* **366**, 170-4 (1993).

7. Mizutani, T. et al. Maintenance of integrated proviral gene expression requires Brm, a catalytic subunit of SWI/SNF complex. *J Biol Chem* **277**, 15859-64 (2002).

8. Reisman, D.N. et al. Concomitant down-regulation of BRM and BRG1 in human tumor cell lines: differential effects on RB-mediated growth arrest vs CD44 expression. *Oncogene* **21**, 1196-207 (2002).

9. Kadam, S. & Emerson, B.M. Transcriptional specificity of human SWI/SNF BRG1 and BRM chromatin remodeling complexes. *Mol Cell* **11**, 377-89 (2003).

10. Mizutani, T. et al. Loss of the Brm-type SWI/SNF chromatin remodeling complex is a strong barrier to the Tat-independent transcriptional elongation of human immunodeficiency virus type 1 transcripts. *J Virol* **83**, 11569-80 (2009).

11. Reisman, D., Glaros, S. & Thompson, E.A. The SWI/SNF complex and cancer. *Oncogene* **28**, 1653-68 (2009).

12. Tando, T. et al. Requiem protein links RelB/p52 and the Brm-type SWI/SNF complex in a noncanonical NF-kappaB pathway. *J Biol Chem* **285**, 21951-60 (2010).

13. Ishizaka, A. et al. Double plant homeodomain (PHD) finger proteins DPF3a and -3b are required as transcriptional co-activators in SWI/SNF complex-dependent activation of NF-κB RelA/p50 heterodimer. *J Biol Chem* **287**, 11924-33 (2012).

14. Yamamichi, N. et al. The Brm gene suppressed at the post-transcriptional level in various human cell lines is inducible by transient HDAC inhibitor treatment,

which exhibits antioncogenic potential. *Oncogene* **24**, 5471-81 (2005).

15. Reisman, D.N., Sciarrotta, J., Wang, W., Funkhouser, W.K. & Weissman, B.E. Loss of BRG1/BRM in human lung cancer cell lines and primary lung cancers: correlation with poor prognosis. *Cancer Res* **63**, 560-6 (2003).

16. Yamamichi, N. et al. Frequent loss of Brm expression in gastric cancer correlates with histologic features and differentiation state. *Cancer Res* **67**, 10727-35 (2007).

17. Shen, H. et al. The SWI/SNF ATPase Brm is a gatekeeper of proliferative control in prostate cancer. *Cancer Res* **68**, 10154-62 (2008).

18. Yamamichi-Nishina, M. et al. SW13 cells can transition between two distinct subtypes by switching expression of BRG1 and Brm genes at the post-transcriptional level. *J Biol Chem* **278**, 7422-30 (2003).

19. Bushati, N. & Cohen, S.M. microRNA functions. *Annu Rev Cell Dev Biol* **23**, 175-205 (2007).

20. Lewis, B.P., Burge, C.B. & Bartel, D.P. Conserved seed pairing, often flanked by adenosines, indicates that thousands of human genes are microRNA targets. *Cell* **120**, 15-20 (2005).

21. Kim, V.N. MicroRNA biogenesis: coordinated cropping and dicing. *Nat Rev Mol*

Cell Biol **6**, 376-85 (2005).

22. Sayed, D. & Abdellatif, M. MicroRNAs in development and disease. *Physiol Rev* **91**, 827-87 (2011).

23. Jansson, M.D. & Lund, A.H. MicroRNA and cancer. *Mol Oncol* **6**, 590-610 (2012).

24. Croce, C.M. Causes and consequences of microRNA dysregulation in cancer. *Nat Rev Genet* **10**, 704-14 (2009).

25. Sakurai, K. et al. MicroRNAs miR-199a-5p and -3p target the Brm subunit of SWI/SNF to generate a double-negative feedback loop in a variety of human cancers. *Cancer Res* **71**, 1680-9 (2011).

26. Shin, S.I., Freedman, V.H., Risser, R. & Pollack, R. Tumorigenicity of virus-transformed cells in nude mice is correlated specifically with anchorage independent growth in vitro. *Proc Natl Acad Sci U S A* **72**, 4435-9 (1975).

27. Pagel, J.I. & Deindl, E. Early growth response 1--a transcription factor in the crossfire of signal transduction cascades. *Indian J Biochem Biophys* **48**, 226-35 (2011).

28. Mariniello, B. et al. Combination of sorafenib and everolimus impacts therapeutically on adrenocortical tumor models. *Endocr Relat Cancer* **19**,

527-39 (2012).

29. Hütz, K. et al. The stem cell factor SOX2 regulates the tumorigenic potential in human gastric cancer cells. *Carcinogenesis* **35**, 942-50 (2014).

30. Shetty, R.S. et al. Synthesis and pharmacological evaluation of N-(3-(1H-indol-4-yl)-5-(2-methoxyisonicotinoyl)phenyl)methanesulfonamide (LP-261), a potent antimitotic agent. *J Med Chem* **54**, 179-200 (2011).

31. Bilsland, A.E. et al. Selective ablation of human cancer cells by telomerase-specific adenoviral suicide gene therapy vectors expressing bacterial nitroreductase. *Oncogene* **22**, 370-80 (2003).

32. Lino Cardenas, C.L. et al. miR-199a-5p Is upregulated during fibrogenic response to tissue injury and mediates TGFbeta-induced lung fibroblast activation by targeting caveolin-1. *PLoS Genet* **9**, e1003291 (2013).

33. Henry, J.C. et al. miR-199a-3p targets CD44 and reduces proliferation of CD44 positive hepatocellular carcinoma cell lines. *Biochem Biophys Res Commun* **403**, 120-5 (2010).

34. Fornari, F. et al. MiR-199a-3p regulates mTOR and c-Met to influence the doxorubicin sensitivity of human hepatocarcinoma cells. *Cancer Res* **70**, 5184-93 (2010).

35. Shatseva, T., Lee, D.Y., Deng, Z. & Yang, B.B. MicroRNA miR-199a-3p regulates cell proliferation and survival by targeting caveolin-2. *J Cell Sci* **124**, 2826-36 (2011).

36. Karantza, V. Keratins in health and cancer: more than mere epithelial cell markers. *Oncogene* **30**, 127-38 (2011).

37. Trask, D.K. et al. Keratins as markers that distinguish normal and tumor-derived mammary epithelial cells. *Proc Natl Acad Sci U S A* **87**, 2319-23 (1990).

38. Ichimi, T. et al. Identification of novel microRNA targets based on microRNA signatures in bladder cancer. *Int J Cancer* **125**, 345-52 (2009).

39. Parton, R.G. & del Pozo, M.A. Caveolae as plasma membrane sensors, protectors and organizers. *Nat Rev Mol Cell Biol* **14**, 98-112 (2013).

40. Zhang, J. et al. Identification of CD44 as a downstream target of noncanonical NF-κB pathway activated by human T-cell leukemia virus type 1-encoded Tax protein. *Virology* **413**, 244-52 (2011).

41. Zhang, X. & Liu, Y. Suppression of HGF receptor gene expression by oxidative stress is mediated through the interplay between Sp1 and Egr-1. *Am J Physiol Renal Physiol* **284**, F1216-25 (2003).

42. Joshi, B. et al. Phosphocaveolin-1 is a mechanotransducer that induces caveola

biogenesis via Egr1 transcriptional regulation. *J Cell Biol* **199**, 425-35 (2012).

43. Matsubara, D. et al. Lung cancer with loss of BRG1/BRM, shows epithelial mesenchymal transition phenotype and distinct histologic and genetic features. *Cancer Sci* **104**, 266-73 (2013).

44. Mangan, S. & Alon, U. Structure and function of the feed-forward loop network motif. *Proc Natl Acad Sci U S A* **100**, 11980-5 (2003).

45. Tsang, J., Zhu, J. & van Oudenaarden, A. MicroRNA-mediated feedback and feedforward loops are recurrent network motifs in mammals. *Mol Cell* **26**, 753-67 (2007).

46. Nowak, D., Stewart, D. & Koeffler, H.P. Differentiation therapy of leukemia: 3 decades of development. *Blood* **113**, 3655-65 (2009).

47. Ito, T. et al. Brm transactivates the telomerase reverse transcriptase (TERT) gene and modulates the splicing patterns of its transcripts in concert with p54(nrb). *Biochem J* **411**, 201-9 (2008).

48. Hoffman, G.R. et al. Functional epigenetics approach identifies BRM/SMARCA2 as a critical synthetic lethal target in BRG1-deficient cancers. *Proc Natl Acad Sci U S A* **111**, 3128-33 (2014).

49. Weinstein, I.B. & Joe, A. Oncogene addiction. *Cancer Res* **68**, 3077-80 (2008).

50. Cheng, C.J. & Slack, F.J. The duality of oncomiR addiction in the maintenance and treatment of cancer. *Cancer J* **18**, 232-7 (2012).

51. Bourguignon, L.Y., Wong, G., Earle, C., Krueger, K. & Spevak, C.C. Hyaluronan-CD44 interaction promotes c-Src-mediated twist signaling, microRNA-10b expression, and RhoA/RhoC up-regulation, leading to Rho-kinase-associated cytoskeleton activation and breast tumor cell invasion. *J Biol Chem* **285**, 36721-35 (2010).

52. Singletary, K. & Ellington, A. Genistein suppresses proliferation and MET oncogene expression and induces EGR-1 tumor suppressor expression in immortalized human breast epithelial cells. *Anticancer Res* **26**, 1039-48 (2006).

53. Ravid, D., Maor, S., Werner, H. & Liscovitch, M. Caveolin-1 inhibits cell detachment-induced p53 activation and anoikis by upregulation of insulin-like growth factor-I receptors and signaling. *Oncogene* **24**, 1338-47 (2005).

54. Kannan, A. et al. Caveolin-1 promotes gastric cancer progression by up-regulating epithelial to mesenchymal transition by crosstalk of signalling mechanisms under hypoxic condition. *Eur J Cancer* **50**, 204-15 (2014).

55. Xu, Y., Stamenkovic, I. & Yu, Q. CD44 attenuates activation of the hippo signaling pathway and is a prime therapeutic target for glioblastoma. *Cancer Res*

70, 2455-64 (2010).

56. Bourguignon, L.Y. Matrix hyaluronan-activated CD44 signaling promotes keratinocyte activities and improves abnormal epidermal functions. *Am J Pathol* **184**, 1912-9 (2014).

57. Bolanos-Garcia, V.M. MET meet adaptors: functional and structural implications in downstream signalling mediated by the Met receptor. *Mol Cell Biochem* **276**, 149-57 (2005).

58. Lloyd, P.G. Caveolin-1, antiapoptosis signaling, and anchorage-independent cell growth. Focus on "Caveolin-1 regulates Mcl-1 stability and anoikis in lung carcinoma cells". *Am J Physiol Cell Physiol* **302**, C1282-3 (2012).

59. Kwon, H., Lee, J., Jeong, K., Jang, D. & Pak, Y. A novel actin cytoskeleton-dependent noncaveolar microdomain composed of homo-oligomeric caveolin-2 for activation of insulin signaling. *Biochim Biophys Acta* **1833**, 2176-89 (2013).

60. Fujisaki, T. et al. CD44 stimulation induces integrin-mediated adhesion of colon cancer cell lines to endothelial cells by up-regulation of integrins and c-Met and activation of integrins. *Cancer Res* **59**, 4427-34 (1999).

61. Elliott, V.A., Rychahou, P., Zaytseva, Y.Y. & Evers, B.M. Activation of c-Met

and upregulation of CD44 expression are associated with the metastatic phenotype in the colorectal cancer liver metastasis model. *PLoS One* **9**, e97432 (2014).

62. Singleton, P.A. et al. CD44 regulates hepatocyte growth factor-mediated vascular integrity. Role of c-Met, Tiam1/Rac1, dynamin 2, and cortactin. *J Biol Chem* **282**, 30643-57 (2007).

63. Mora, R. et al. Caveolin-2 localizes to the golgi complex but redistributes to plasma membrane, caveolae, and rafts when co-expressed with caveolin-1. *J Biol Chem* **274**, 25708-17 (1999).

64. Tatarelli, C., Linnenbach, A., Mimori, K. & Croce, C.M. Characterization of the human TESTIN gene localized in the FRA7G region at 7q31.2. *Genomics* **68**, 1-12 (2000).

65. Watanabe, H. et al. SWI/SNF complex is essential for NRSF-mediated suppression of neuronal genes in human nonsmall cell lung carcinoma cell lines. *Oncogene* **25**, 470-9 (2006).

66. Haraguchi, T. et al. SiRNAs do not induce RNA-dependent transcriptional silencing of retrovirus in human cells. *FEBS Lett* **581**, 4949-54 (2007).

67. Yamamichi, N. et al. Locked nucleic acid in situ hybridization analysis of

miR-21 expression during colorectal cancer development. *Clin Cancer Res* **15**, 4009-16 (2009).